ELSEVIER

Contents lists available at ScienceDirect

European Journal of Mechanics / A Solids

journal homepage: www.elsevier.com/locate/ejmsol





Displacement-driven approach to nonlocal elasticity

Sansit Patnaik a,*, Sai Sidhardh a,b, Fabio Semperlotti a,*

- a Ray W. Herrick Laboratories, School of Mechanical Engineering, Purdue University, West Lafayette, IN 47907, USA
- b Department of Mechanical and Aerospace Engineering, Indian Institute of Technology, Hyderabad, Kandi, TG 502285, India

ARTICLE INFO

Keywords:
Nonlocal elasticity
Integral methods
Displacement-driven approach
Energy methods
Nonlocal beams
Nonlocal plates

ABSTRACT

This study presents a physically-consistent displacement-driven reformulation of the concept of action-at-adistance, which is at the foundation of nonlocal elasticity. In contrast to the class of existing approaches that adopts an integral stress-strain constitutive relation, the displacement-driven approach is predicated on an integral strain-displacement relation. One of the most remarkable consequence of this reformulation is that the (total) strain energy is guaranteed to be a convex and positive-definite function without imposing any constraint on the symmetry of the nonlocal kernel. This feature is critical to enable the application of nonlocal formulations to general continua exhibiting asymmetric interactions; ultimately a manifestation of material heterogeneity. Remarkably, the proposed approach also enables a strong (point-wise) satisfaction of the locality recovery condition and of the laws of thermodynamics, which are not foregone conclusions in most classical nonlocal elasticity theories. Additionally, the formulation is frame-invariant and the nonlocal operator remains physically consistent at material interfaces and domain boundaries. The study is complemented by a detailed analysis of the dynamic response of the nonlocal continuum and of its intrinsic dispersion, leading to the consideration that the choice of a nonlocal kernel should depend on the specific material. Examples of either exponential or power-law kernels are presented in order to demonstrate the applicability of the method to different classes of nonlocal media. The ability to admit generalized kernels reinforces the generalized nature of the displacement-driven approach over existing integral methodologies, which typically lead to simplified differential models based on exponential kernels. The theoretical formulation is also leveraged to perform numerical simulations of the linear static response of nonlocal beams and plates further illustrating the intrinsic consistency of the approach, which is free from unwanted and unrealistic boundary effects.

1. Introduction

Experimental and theoretical investigations have shown that, irrespective of the spatial scale, size-dependent effects or nonlocal effects can become prominent in the response of several structures in the most diverse fields of engineering, nanotechnology, biotechnology, and even medicine (Eringen, 1972; Romanoff and Reddy, 2014; Romanoff et al., 2020; Patnaik et al., 2021a; Alotta et al., 2020; Zhu et al., 2020). The study and analysis of nonlocal effects has increasingly become an important component of structural design and analysis. Specific examples of size-dependent structures include sensors, biological implants, micro/nano-electromechanical devices, and even macroscale structures such as stiffened or sandwiched panels in naval and aerospace applications (Zhu et al., 2020; Alotta et al., 2020; Nair, 2019; Pradhan and Murmu, 2009; Romanoff et al., 2020; Patnaik et al., 2021a). In the case of micro- and nano-structures, for example those involving carbon nanotubes or graphene sheets, nonlocal effects can be traced back to interatomic interactions, and even medium heterogeneity (Pradhan and

Murmu, 2009; Wang et al., 2011; Trovalusci et al., 2017; Tuna et al., 2019; Patnaik et al., 2021b; Lal and Dangi, 2019). These nonlocal forces operate at the nanoscale and hence do not significantly contribute to the overall macroscopic response. For these reasons, nonlocal effects have long been considered negligible at the macro scales. However, at the macro scales, nonlocal effects can originate from material heterogeneities (Bazant, 1976; Romanoff and Reddy, 2014; Trovalusci et al., 2014; Patnaik and Semperlotti, 2020a; Alotta et al., 2020; Romanoff et al., 2020; Hollkamp and Semperlotti, 2020; Patnaik et al., 2021a) or even from intentionally nonlocal designs (Nair, 2019; Zhu et al., 2020). While long-range interactions occur naturally in heterogeneous materials (e.g. interactions between the layers of a functionally graded material), they can also be induced artificially via carefully designed structural links in the intentional nonlocal designs. The existence of size-dependent effects leads to a softening or stiffening of the structure when compared to the predictions made from the classical (local) continuum mechanics formulation. Additionally, size-dependent structures

E-mail addresses: spatnai@purdue.edu (S. Patnaik), fsemperl@purdue.edu (F. Semperlotti).

^{*} Corresponding authors.

exhibit anomalous wavenumber–frequency dispersion characteristics leading to wavenumber/frequency dependent wave speeds, contrary to constant wave speeds achieved via local descriptions (Fellah et al., 2004a; Buonocore et al., 2019; Fellah et al., 2004b; Patnaik and Semperlotti, 2020a; Hollkamp and Semperlotti, 2020). Consequently, the ability to accurately model size-dependent effects has profound implications for the diverse applications in the aforementioned examples. The inability of the classical continuum theory in capturing size-dependent effects prevented its use in these types of applications and led to the development of nonlocal continuum theories.

Seminal studies by Kröner (1967), Edelen and Laws (1971), and Eringen and Edelen (1972), Eringen (1972) laid the theoretical foundation of nonlocal elasticity, and explored its role in the modeling of nonlocal size-dependent structures. The mathematical description of the nonlocal continuum theories proposed in these seminal studies relied on the introduction of additional contributions, resulting from long-range nonlocal interactions, in terms of a convolution integral of the strain field in the constitutive equations. Over the years, several researchers (Silling, 2000; Lazopoulos, 2006; Di Paola et al., 2013; Pisano et al., 2021; Romano and Barretta, 2017; Rahimi et al., 2017) have proposed different modifications to the formulations presented in the seminal studies (Kröner, 1967; Edelen and Laws, 1971; Eringen and Edelen, 1972). From a mathematical standpoint, these approaches belong to a class of the so-called strong integral methods that capture nonlocal effects by re-defining the stress-strain constitutive law in the form of a convolution integral of either the strain or the stress field over a certain spatial domain (the so-called horizon of nonlocality). Depending on whether the nonlocal contributions are modeled using the strain or the stress field, the integral method can be classified as a stressdriven (Romano and Barretta, 2017) or a strain-driven (Polizzotto, 2001; Polizzotto et al., 2004, 2006) approach. Further discussions on the origin of nonlocal effects, existing theories of nonlocal elasticity, and their applications can be found in this recent review study (Shaat et al., 2020).

Although the strain- and stress-driven integral approaches to nonlocal elasticity have been able to address a multitude of aspects typical of the response of size-dependent nonlocal structures, some important challenges still remain open. In both these approaches, the nonlocal continuum formulation is based on a nonlocal definition of the stress–strain constitutive relation and a local definition of the strain-displacement kinematic relation. In other terms, the effect of nonlocality is accounted only via the constitutive stress–strain relations. Indeed, we will show that it is this assumption that is at the root of several of the challenges faced by the existing approaches. These challenges are summarized in the following:

· The strain-driven approach leads to a Fredholm integral of the first-kind, which results in ill-posed boundary-value problems. Consequently, its application to model nonlocal structures of practical engineering interest (e.g. beams) leads to inconsistent (also called 'paradoxical') predictions when the same analysis is performed under different loading conditions (Challamel and Wang, 2008; Fernández-Sáez et al., 2016; Romano et al., 2017). The issue of an ill-posed formulation was addressed by adopting either a mixed-phase (local and nonlocal) approach (Pisano et al., 2021; Eroglu, 2020) or a stress-driven approach (Romano and Barretta, 2017), which led to nonlocal constitutive boundary conditions. Mathematically speaking, these nonlocal constitutive boundary conditions are additional constraints required to guarantee wellposedness of the integral equations. Notably, the stress-driven approach is yet to achieve a practical numerical implementation (e.g. finite element method) and currently relies on analytical methods to simulate the nonlocal response. While the analytical approach does provide interesting insights, it prevents the application of the stress-driven theory to more complex scenarios involving, as an example, higher dimensional structures subject to general loading conditions or nonlinear behavior.

- Further, the most direct result of adopting either the strain- or the stress-driven constitutive formulation consists in the inability to achieve a positive-definite and convex strain energy density. This follows from the fact that the strain energy density consists of the product between a function and its convolution with a kernel, which does not yield a quadratic form. Consequently, the only route to achieve a positive-definite (total) strain energy is to require a symmetric nonlocal kernel (Polizzotto, 2001; Romano and Barretta, 2017). While possible, such a condition restricts the application of the resulting theory to structures exhibiting asymmetric long-range interactions (Askari et al., 2008; Trovalusci et al., 2014, 2017; Zhu et al., 2020; Sumelka, 2017). This aspect was also discussed very recently in Batra (2021), which highlighted the misuse of Eringen's stress–strain nonlocal constitutive relation to model functionally graded structures.
- In addition to the restriction on the symmetry of the convolution kernel, several studies also restrict the functional nature of the kernel. More specifically, most strain- and stress-driven integral approaches reduce to simplified differential models using the special exponential kernel (Pradhan and Murmu, 2009; Askes and Aifantis, 2011; Wang et al., 2011; Romano and Barretta, 2017; Lal and Dangi, 2019). The use of an exponential kernel, while being a plausible option, prevents the application of the resulting theory to a wide class of structures, particularly those exhibiting anomalous attenuation and dispersion (as we will show in Section 6). Examples include highly scattering and multifractal media (Fellah et al., 2004a; Hollkamp et al., 2019; Buonocore et al., 2019; Hollkamp and Semperlotti, 2020), biological media (Fellah et al., 2004b; Magin, 2010), and structures with intentionally designed nonlocal connections (Nair, 2019; Zhu et al., 2020).
- The use of a nonlocal stress–strain constitutive relation violates the locality recovery condition which states that, for a physically consistent nonlocal formulation, a uniform stress field and a length-scale independent strain energy must be recovered from a uniform strain field (Polizzotto et al., 2006). Notably, this limitation was addressed very recently in Pisano et al. (2021) via an enhanced mixed-phase model, albeit in a weaker form that satisfies only the local stress recovery condition.
- As noted in Polizzotto et al. (2004), the use of a nonlocal stressstrain constitutive behavior is not robust to boundary and surface effects in finite domains. This is a direct result of an inconsistent (and incomplete) truncation of the nonlocal kernel (often, exponential) at boundaries.

Some of the above mentioned challenges are also described in Pisano et al. (2021). In this study, we attempt to address these conceptual as well as practical limitations of the existing approaches to non-local elasticity via fundamental changes in the nonlocal constitutive modeling. More specifically, we reformulate the concept of action-at-a-distance by using nonlocal kinematic relations with a generalized kernel (not restricted to exponential functions). We analyze the specific advantages of the proposed approach and illustrate how this method is well equipped to address the different challenges faced by existing integral approaches.

The concept of nonlocal kinematics can be traced back to a seminal study of Drapaca et al. on modeling nonlocal solids by using fractional calculus (Drapaca and Sivaloganathan, 2012). Fractional-order operators are a class of differ-integral operators, uniquely equipped to model temporal and spatial memory effects in complex materials (Carpinteri et al., 2014; Mashayekhi et al., 2018; Failla and Zingales, 2020; Magin, 2010; Lazopoulos and Lazopoulos, 2020). The authors in Drapaca and Sivaloganathan (2012) reformulated the classical (local) deformation gradient tensor by using fractional-order derivatives and used the fractional deformation gradient tensor to build the nonlocal continuum theory. This approach was later refined by Sumelka in Sumelka (2014, 2017) and applied to the analysis of slender engineering structures.

A key limitation of the above mentioned studies (Drapaca and Sivaloganathan, 2012; Sumelka, 2014) consists in an ad-hoc imposition of force and moment balance principles. The governing equations in these studies were derived by a direct replacement of the local stress tensor (in the classical continuum governing equations) with the nonlocal stress tensor. However, as shown in Polizzotto (2001), the application of global balance principles to derive governing equations with nonlocal operators leads to the presence of (additional) integral terms. Further, the traction boundary conditions in these studies were identical to Cauchy's postulate for surface tractions. The presence of nonlocal interactions however, leads to a modification of Cauchy's postulate resulting in nonlocal traction conditions (Dell'Isola et al., 2012, 2015; Sidhardh et al., 2021a). A significant benefit of adopting fractional-order (nonlocal) kinematics was exposed in Patnaik et al. (2020b, 2021c,a), where the authors could define a positive-definite nonlocal continuum formulation ultimately enabling the use of variational principles. This latter approach had both theoretical advantages including the formulation of well-posed governing equations (Patnaik et al., 2020b, 2021c), the incorporation of nonlinear effects (Sidhardh et al., 2020; Patnaik et al., 2020c; Sidhardh et al., 2021b), thermodynamic consistency (Sidhardh et al., 2021a), as well as practical implications like the ability to develop finite element solutions (Patnaik et al., 2020b, 2021c). These advantages allowed the application of the fractional-order kinematic approach to model the response of different nonlocal structures subject to mechanical and thermomechanical loading conditions (Patnaik et al., 2021a; Patnaik and Semperlotti, 2020a). In all the above mentioned studies, consistent predictions free from boundary and loading effects were obtained.

In this study, we extend the fractional-order kinematic approach proposed in Drapaca and Sivaloganathan (2012), Sumelka (2014), Patnaik and Semperlotti (2020a) and Patnaik et al. (2021b), to develop a generalized and well-posed nonlocal kinematic approach. In the following, we will refer to this approach as the *displacement-driven approach to nonlocal elasticity*. Broadly speaking, this approach uses a general differ-integral (nonlocal) definition to capture the strain-displacement relations of a nonlocal continuum. It is exactly this feature that allows the displacement-driven approach to overcome the limitations of existing integral approaches. The process of formulating the displacement-driven approach, analyzing its characteristics, and exploring its application, can be divided into three main tasks:

- First, we will develop the displacement-driven approach to nonlocal elasticity based on generalized nonlocal (differ-integral) operators introduced within the classical (local) strain–displacement relation. This approach leads to a convex and positive-definite formulation without requiring a symmetric kernel. In this process, we will also analyze the satisfaction of the locality recovery condition, the frame-invariance of the formulation, and the consistent behavior of the nonlocal operator at boundaries. We will complete the analysis of the displacement-driven continuum approach by casting the formulation within a thermodynamic framework and demonstrating its thermodynamic consistency. In this regard, we will show how this approach allows a strong (point-wise) imposition of thermodynamic balance laws, consistent with the principles of thermodynamics.
- Following the development of the displacement-driven constitutive relations, we will derive the equilibrium equations describing the response of the nonlocal solid by using variational principles. Further, we will derive dispersion relations describing the transient dynamics of the nonlocal bulk solid. By taking the example of either an exponential or a power-law kernel, we will demonstrate how the specific choice of the kernel should not be universal but rather determined based on experimental dispersion characteristics carrying the signature of the specific material.

• Finally, we will apply the displacement-driven approach to model the linear static response of nonlocal beams and plates. For this purpose, we will employ the shear-deformable Timoshenko beam and Mindlin plate models. Since the Euler-Bernoulli beam and the Kirchhoff plate formulations can be recovered as special cases from the Timoshenko and Mindlin formulations, the latter choice allows obtaining more general results. Using a finite element procedure, we will numerically simulate the response of the structural elements for various combinations of nonlocal kernels, kernel parameters, and loading conditions. The choice of using a finite element based solver follows from the flexibility afforded by this method in dealing with general loading conditions as well as integral boundary conditions, typical of nonlocal models (Polizzotto, 2001; Patnaik et al., 2021b). The numerical results will show that the displacement-driven approach predicts a consistent softening behavior irrespective of the nature of the kernel and loading conditions. Further, we will provide some broad discussions highlighting the capability of the developed approach in modeling stiffening effects, nonlinear effects, and physical phenomena involving the propagation of discontinuities (e.g. fracture and impact).

The remainder of the paper is structured as follows: first we discuss the formulation and the relevance of nonlocal elasticity via the displacement-driven approach in Section 2. The analysis of the frame-invariance of the formulation and of the behavior of the nonlocal operator at boundaries follows in Section 3. We discuss the thermodynamic consistency of the formulation in Section 4. In Section 5, we derive the governing equations for the displacement-driven approach. We derive the dispersion relations for a 1D nonlocal bulk solid in Section 6 and use the relations to discuss the importance of adopting material-informed kernels. Finally, we apply the proposed approach to model the linear static response of nonlocal beams and plates in Section 7.

2. Reformulation of nonlocal elasticity: Displacement-driven approach

As mentioned in the introduction, the motivation to reformulate the classical approaches to nonlocal elasticity follows from the non-convex nature of the strain energy density obtained via these approaches. To better highlight this aspect, we first provide a brief review of the classical integral approaches to nonlocal elasticity.

In the classical approaches (either strain- or stress-driven) to nonlocal elasticity, the stress and strain at a given point within the nonlocal continuum are related by an integral (convolution) operator. This integral operator enriches the response of a point with the information of the response of a collection of points located within a characteristic distance known as the *horizon of nonlocality*. Depending on the specific approach, the stress–strain constitutive relation consists of the convolution of a spatially (monotonically) decaying kernel with either the strain (Eringen and Edelen, 1972; Polizzotto, 2001) or the stress (Romano and Barretta, 2017) field in the following fashion:

Strain-driven approach:
$$\sigma_{ij}(\mathbf{x}) = \int_{\Omega} \mathbb{C}_{ijkl} \mathcal{K}_{\varepsilon}(\mathbf{x}, \mathbf{x}') \varepsilon_{kl}(\mathbf{x}') d\mathbf{x}'$$
 (1a)

Stress-driven approach:
$$\epsilon_{ij}(\mathbf{x}) = \int_{\overline{\Omega}} \mathbb{S}_{ijkl} \mathcal{K}_{\sigma}(\mathbf{x}, \mathbf{x}') \sigma_{kl}(\mathbf{x}') d\mathbf{x}'$$
 (1b)

where $\sigma_{ij}(x)$ and $\varepsilon_{ij}(x)$ denote the stress and strain tensor at a point x within the domain of the solid Ω , and x' is a point within the horizon of nonlocality $\overline{\Omega} \subseteq \Omega$. $\mathbb C$ and $\mathbb S$ are the fourth-order material elasticity and compliance tensors, respectively. $\mathcal K_\varepsilon(x,x')$ and $\mathcal K_\sigma(x,x')$ are the nonlocal kernels that determine the strength of the long-range interactions between the points x and x', in the strain- and stress-driven approaches, respectively.

The constitutive relations in Eq. (1) result in the following expressions for the total strain energy (Π) and the strain energy density ($\mathbb{U}(x)$) of the nonlocal solid (Polizzotto, 2001; Romano and Barretta, 2017):

Strain-driven approach:

$$\Pi = \frac{1}{2} \int_{\Omega} \underbrace{\left[\varepsilon_{ij}(\mathbf{x}) \int_{\overline{\Omega}} \mathbb{C}_{ijkl} \mathcal{K}_{\varepsilon}(\mathbf{x}, \mathbf{x}') \varepsilon_{kl}(\mathbf{x}') d\mathbf{x}' \right]}_{\mathbb{U}(\mathbf{x})} d\mathbf{x}$$
 (2a)

Stress-driven approach:

$$\Pi = \frac{1}{2} \int_{\Omega} \left[\sigma_{ij}(\mathbf{x}) \int_{\overline{\Omega}} \mathbb{S}_{ijkl} \mathcal{K}_{\sigma}(\mathbf{x}, \mathbf{x}') \sigma_{kl}(\mathbf{x}') d\mathbf{x}' \right] d\mathbf{x}$$
 (2b)

It appears from the above expressions that, in either the strain- or stress-driven approach, the strain energy density cannot be reduced to a quadratic form, and hence it is not always guaranteed to be positivedefinite. While it is possible to achieve a positive value for the total strain energy, this imposes restrictions on the nature of the kernel, that is, the kernel must be positive and symmetric in nature (Polizzotto, 2001; Romano and Barretta, 2017). It was argued, in the introduction, that this latter requirement on symmetry can prevent the application of the resulting theory to several cases of practical relevance (Batra, 2021). As an example, consider a collection of particles that is either heterogeneous or subject to thermal gradients. In such case, the interactions on either side of a given particle are not symmetric (Askari et al., 2008; Trovalusci et al., 2014, 2017; Zhu et al., 2020; Batra, 2021; Sumelka, 2017), hence violating the assumption of a symmetric kernel. In other terms, from a physical perspective, the assumption of a symmetric kernel can be considered valid only for isotropic structures with an underlying symmetry in the arrangement of particles (Tuna et al., 2019). Mathematically speaking, the restriction of a symmetric kernel is a direct result of the fact that the strain energy density functional is not guaranteed to be positive or convex in nature (simply because it consists of the product of the integral of a function and the function itself, which is not always convex in nature). As noted in classical (local) continuum mechanics, a well-posed elastostatic formulation is guaranteed iff the strain energy density is both convex and positive-definite in nature.

A possible route to achieve a convex and positive-definite formulation consists in maintaining the quadratic form of the strain energy density, analogous to local elastic continuum mechanics, such that the stress is a work-conjugate of the strain:

$$\mathbb{U} = \frac{1}{2}\sigma_{ij}\varepsilon_{ij} \equiv \frac{1}{2}\mathbb{C}_{ijkl}\varepsilon_{ij}\varepsilon_{kl} \equiv \frac{1}{2}\mathbb{S}_{ijkl}\sigma_{ij}\sigma_{kl}$$
 (3)

The use of the above quadratic form for the strain energy density requires nonlocality to be introduced directly into the strain tensor, or equivalently into the stress tensor, while using a non-integral stress-strain constitutive relation. Indeed, this can be achieved by insisting that the strain–displacement (kinematic) relations are nonlocal (differintegral) in nature while the stress–strain constitutive relation follow the local continuum formulation. By following the latter argument, we define the infinitesimal strain tensor and the Cauchy stress tensor as:

$$\varepsilon = \frac{1}{2} \left[\overline{\nabla} u + \overline{\nabla} u^T \right] \tag{4a}$$

$$\sigma = \mathbb{C} : \varepsilon$$
 (4b)

where u(x) is the displacement field. $\overline{\mathbf{v}}$ is a differ-integral gradient operator defined as:

$$\overline{\nabla}(\cdot) = \overline{D}_{x}(\cdot)\hat{x} + \overline{D}_{y}(\cdot)\hat{y} + \overline{D}_{z}(\cdot)\hat{z}$$
(5)

where $\{\hat{x},\hat{y},\hat{z}\}$ are the Cartesian basis vectors. $\overline{D}_{x_j}(\cdot)$ is a differ-integral operator similar to the convolution operations in Eq. (1) and is defined in the following manner:

$$\overline{D}_{x_j} \phi = \int_{\overline{\Omega}_j} c_j^* \mathcal{K}(\mathbf{x}, \mathbf{x}') \left[D_{x_j'}^1 \phi \right] \mathrm{d}x_j'$$
 (6)

where ϕ is an arbitrary function. c_j^* is a scalar multiplier for the differintegral operator in the \hat{x}_j direction, which will be used to enforce frame-invariance and dimensional consistency of the formulation in Section 3. $\mathcal{K}(x,x')$ denotes the nonlocal kernel of the displacement-driven approach. Further, $D_{x_j'}^1 \phi$ indicates the classical first-order deriva-

tive $\mathrm{d}\phi/\mathrm{d}x_j'$. For a nonlocal horizon $\overline{\Omega}_j = [x_{-j}, x_{+_j}]$ in the \hat{x}_j direction about the point x, the nonlocal operator can be expanded as:

$$\overline{D}_{x_j}\phi = c_{-j}^* \int_{x_{-i}}^{x_j} \mathcal{K}(\mathbf{x}, \mathbf{x}') \left[D_{x_j'}^1 \phi \right] \mathrm{d}x_j' + c_{+j}^* \int_{x_i}^{x_{+j}} \mathcal{K}(\mathbf{x}, \mathbf{x}') \left[D_{x_j'}^1 \phi \right] \mathrm{d}x_j' \quad (7)$$

where c_{-j}^* and c_{+j}^* are independent scalar multipliers. The length of the horizon of nonlocality on either side of the point \mathbf{x} in the \hat{x}_j direction are denoted as I_{-j} and I_{+j} , such that $I_{-j} = x_j - x_{-j}$ and $I_{+j} = x_{+j} - x_j$. In general, $I_{-j} \neq I_{+j}$ implying that the horizon of nonlocality is not necessarily symmetric, like in cases involving material interfaces or boundaries falling within the horizon. This aspect is schematically illustrated in Fig. 1.

Revisiting the strain energy density of the nonlocal solid obtained via the proposed constitutive formulation, we obtain:

$$\mathbb{U} = \frac{1}{2} \underbrace{C_{ijkl} \left[\overline{D}_{x_j} u_i + \overline{D}_{x_i} u_j \right]}_{\text{Nonlocal stress}} \underbrace{\left[\overline{D}_{x_l} u_k + \overline{D}_{x_k} u_l \right]}_{\text{Nonlocal strain}} \tag{8}$$

which immediately demonstrates its convex nature, irrespective of whether the nonlocal kernel is symmetric or asymmetric in nature. We denominate this nonlocal approach as the "displacement-driven approach to nonlocal elasticity" since nonlocality is embedded via the nonlocal strain–displacement kinematic relations Eq. (4a). Note that the stress-strain constitutive relations in Eq. (4b) are non-integral in nature contrary to the classical stress- and strain-driven approaches to nonlocal elasticity (Polizzotto, 2001; Romano and Barretta, 2017). Remarkably, this functional form for the stress–strain constitutive relation trivially satisfies the locality recovery condition (Polizzotto et al., 2006). More specifically, it ensures that a uniform strain field induces a uniform stress field, and consequently, we obtain a length-scale independent strain energy density via Eq. (3).

The displacement-driven formulation deserves some additional remarks. While the approach was presented starting on strain energy arguments, the same formulation can be derived via standard continuum mechanics arguments. In this study, we favored the former approach to clearly highlight the connection to a convex and positive-definite nonlocal formulation. When following a continuum mechanics approach, the displacement-driven formulation can be derived by starting from a nonlocal deformation gradient tensor which relates the differential line elements in the deformed and undeformed configurations by using the differ-integral gradient operator defined in Eq. (5). More specifically, the nonlocal deformation gradient tensor, which maps a differential element in the undeformed configuration to the deformed configuration, can be defined as:

$$\overline{F}_{ij} = \overline{D}_{X_i} x_i \tag{9}$$

where X and x denote points within the undeformed and deformed coordinates, respectively. Following the above definition for the nonlocal deformation gradient tensor, a fully nonlinear Lagrangian and Eulerian description of the strain tensor can be derived by using the scalar difference of the differential line elements in the deformed and undeformed configurations, similar to classical continuum formulation. The same approach, albeit by using specialized power-law kernels, which transforms the gradient operator in Eq. (5) into a nonlocal gradient operator containing the well established fractional-order derivatives, can be found in Drapaca and Sivaloganathan (2012), Sumelka (2014) and Patnaik and Semperlotti (2020a).

Note that the model relies on the important hypothesis of nonlocal kinematics. While this hypothesis might appear unsettling in the context of the more classical continuum approaches, we emphasize that

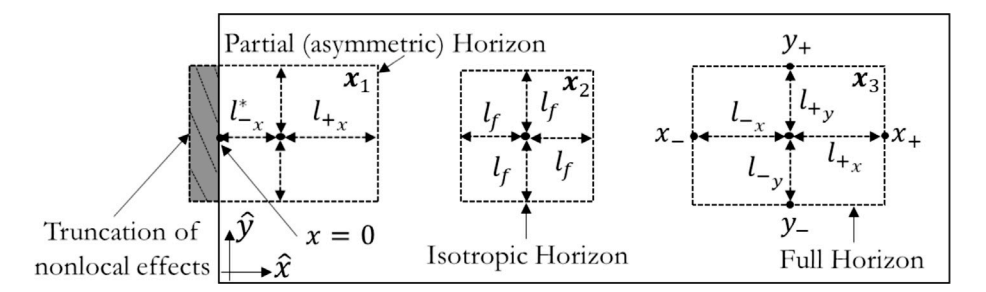


Fig. 1. Schematic illustration of the horizon of nonlocality at different points in a 2D domain. In general, for a domain characterized by asymmetric interactions, $l_{-j} \neq l_{+j}$, and for a domain characterized by anisotropic interactions, $l_{-j} \neq l_{-j}$ ($\square \in \{-,+\}$). These general cases, corresponding to the point x_3 , are denoted as the full horizon. In the case of a domain characterized by symmetric nonlocal interactions (see x_2), the horizon of nonlocality is equal to l_f on either sides in all the directions. However, the horizon of nonlocality must be truncated due to the presence of boundaries. As an example, the horizon is truncated at x_1 , such that $l_{-x}^* < l_{+x}$. In a similar way, it follows that for a point located on the boundary x = 0 it must be $l_- = 0$.

such definition is simply a reformulation of the concept of *action-ata-a-distance*. This hypothesis results in assuming that the response of a selected point within the solid is affected directly by the response of a collection of points within the horizon of nonlocality. Given that the differ-integral operator is applied directly to the displacement field, from a physical standpoint, the formulation accounts for long-range interactions that are proportional to the relative displacement of distant points within the horizon. Recall that, in the continuum description of the displacement-driven approach, differential line elements are defined using nonlocal deformation gradients. It follows that, a change in length of an infinitesimal line at the point x, between the undeformed and the deformed configurations, would be affected directly by the response of the points within the nonlocal horizon of x. This is indeed a reformulation of action-at-a-distance that is often implemented in terms of long-range forces.

3. Frame-invariance: Enforcement and implications

The reformulation of the kinematic relations via differ-integral operators requires a thorough investigation of frame-invariance which states that a rigid-body motion should not induce a change in the strain energy. In this section, we derive expressions for the scalar multipliers $\{(c_-^*, c_+^*)\}$ such that frame-invariance is satisfied at all points within the nonlocal continuum. Remarkably, the satisfaction of frame-invariance via the scalar multipliers also ensures dimensional consistency of the formulation and a consistent behavior of the nonlocal operator at material boundaries.

3.1. Enforcing frame-invariance

Consider the following rigid-body motion superimposed on the undeformed configuration of the body:

$$\chi(X,t) = C(t) + Q(t)X, \tag{10}$$

where C(t) is a spatially constant term representing a translation and Q(t) is a proper orthogonal tensor denoting a rotation. Under this rigid-body motion, the deformation gradient tensor \overline{F}^{χ} should be an orthogonal tensor such that $\overline{F}^{\chi T} \overline{F}^{\chi} = \mathbf{I}$. More specifically, the nonlocal deformation gradient tensor should transform as $\overline{F}^{\chi} = Q$ in order to ensure that the strain measures corresponding to the rigid-body motion are null. From the definition of \overline{F}^{χ} given in Eq. (9) it follows that:

$$\overline{D}_{x_j} \chi_i = c_{-j}^* \int_{x_{-j}}^{x_j} \mathcal{K}(\bm{x}, \bm{x}') D^1_{x_j'} \chi_i(\bm{x}', t) \mathrm{d}x_j' + c_{+j}^* \int_{x_j}^{x_{+j}} \mathcal{K}(\bm{x}, \bm{x}') D^1_{x_j'} \chi_i(\bm{x}', t) \mathrm{d}x_j'$$

Further, noting that $D^1_{x_i'}C_i(t)=0$ and $\mathbf{Q}=\mathbf{Q}(t)$, we obtain:

$$D_{x'_{i}}^{1}\chi_{i}(x',t) = Q_{ik}x_{k,j} = Q_{ik}\delta_{kj} = Q_{ij}$$
 (12)

Thus, under the rigid body motion χ :

$$\overline{D}_{x_j} \chi_i = \left[c_{-j}^* \int_{x_{-i}}^{x_j} \mathcal{K}(\mathbf{x}, \mathbf{x}') dx_j' + c_{+j}^* \int_{x_j}^{x_{+j}} \mathcal{K}(\mathbf{x}, \mathbf{x}') dx_j' \right] Q_{ij}$$
 (13)

To achieve frame-invariance, that is, enforcing $\overline{D}_{x_j}\chi_i=Q_{ij}$ at all points within the continuum for all time instants, we require that:

$$\{c_{-j}^*, c_{+j}^*\} = \left\{ \frac{1}{2 \int_{x_{-j}}^{x_j} \mathcal{K}(\mathbf{x}, \mathbf{x}') d\mathbf{x}'_j}, \frac{1}{2 \int_{x_j}^{x_{+j}} \mathcal{K}(\mathbf{x}, \mathbf{x}') d\mathbf{x}'_j} \right\}$$
(14)

Notably, the above expressions for c_{-j}^* and c_{+j}^* also ensure the dimensional consistency of the formulation.

Here below we provide the expressions of $\{c_{-j}^*, c_{+_j}^*\}$ for some kernels commonly adopted in literature:

• Exponential kernel: $\mathcal{K}(\mathbf{x}, \mathbf{x}') = \exp\left(-\frac{|\mathbf{x}-\mathbf{x}'|}{l_0}\right)$, where l_0 is a material parameter:

$$\{c_{-j}^*, c_{+j}^*\} = \left\{ \frac{1}{2l_0} \left[1 - \exp\left(-\frac{l_{-j}}{l_0}\right) \right]^{-1}, \ \frac{1}{2l_0} \left[1 - \exp\left(-\frac{l_{+j}}{l_0}\right) \right]^{-1} \right\}$$
(15)

• *Power-law kernel:* $\mathcal{K}(\mathbf{x}, \mathbf{x}') = |\mathbf{x} - \mathbf{x}'|^{-\alpha} / \Gamma(1 - \alpha)$, where $\Gamma(\cdot)$ is the well known Gamma function and $\alpha \in (0, 1]$ is a material parameter:

$$\{c_{-j}^*, c_{+j}^*\} = \left\{ \frac{1}{2} \Gamma(2 - \alpha) l_{-j}^{\alpha - 1}, \frac{1}{2} \Gamma(2 - \alpha) l_{+j}^{\alpha - 1} \right\}$$
 (16)

We merely note that, by assuming the above power-law form for the nonlocal kernel, and substituting the corresponding expressions of $\{c_{-j}^*, c_{+j}^*\}$ in Eq. (7), we recover the definition of the Riesz–Caputo fractional-order derivative as presented in Patnaik and Semperlotti (2020a). Consequently, the fractional-order approach to nonlocal elasticity presented in Patnaik and Semperlotti (2020a) can be recovered from the displacement-driven approach, as a special case.

While the above results are limited to the exponential and the power-law kernels, the approach is general and can be extended to other nonlocal kernels such as, for example, bell and conical curves employed in classical strain- and stress-driven models of nonlocal elasticity (Polizzotto, 2001). In each case, the constants c_{+}^{*} and c_{+}^{*} must be derived by using Eq. (14). We will analyze the specific impact of different nonlocal kernels in more detail in Section 6.

3.2. Behavior of the nonlocal operator at boundaries

A detailed analysis of the expressions for the scalar multipliers c_{-j}^* and c_{+}^* in Eq. (14) presents some interesting insights on the nature of

(11)

the kernel at material boundaries that will be of practical relevance. For the most general definition of the kernel $\mathcal{K}(x, x')$ and the location of the point x, recall that, $l_{-i} \neq l_{+i}$. It immediately follows from Eq. (14) that $c_{-}^* \neq c_{+}^*$. This latter condition, apart from ensuring an exact satisfaction of frame-invariance, also ensures the completeness of the nonlocal kernel at points close to the material boundaries or at points located on the boundary itself. In order to demonstrate this latter aspect, we investigate the behavior of the nonlocal operator $\overline{D}_{x_i}\phi$ at a point located on the boundary of the nonlocal solid given in Fig. 1.

For a point (say x_0) located on one of the boundaries (identified by the normal in the *j*th direction), either $l_{-j} \to 0$ or $l_{+j} \to 0$ (see Fig. 1). Here below we present the expression for the nonlocal operator when $l_{-j} \to 0$ (similar expressions hold when $l_{+j} \to 0$). This limiting case, upon using the expression for c_{-j}^* in Eq. (14), gives:

$$\lim_{l_{-j} \to 0} \overline{D}_{x_{j}} \phi = \lim_{l_{-j} \to 0} \left[\frac{1}{2 \int_{x_{0j} - l_{-j}}^{x_{0j}} \mathcal{K}(\mathbf{x}, \mathbf{x}') dx'_{j}} \int_{x_{0j} - l_{-j}}^{x_{0j}} \mathcal{K}(\mathbf{x}, \mathbf{x}') D_{x'_{j}}^{1} \phi dx'_{j} + c_{+j}^{*} \int_{x_{0j}}^{x_{+j}} \mathcal{K}(\mathbf{x}, \mathbf{x}') D_{x'_{j}}^{1} \phi dx'_{j} \right]$$
(17)

Since the interval length (= l_{-i}) of the left integral within the righthand side of the above equation is infinitesimal, D^1 , ϕ can be assumed to be constant within the left integral, and equal to the boundary

$$D_{x_{i}}^{1}\phi = D_{x_{i}}^{1}\phi\Big|_{x_{0}} \tag{18}$$

Substituting Eq. (18) in Eq. (17) leads to Eq. (19) in Box I. Eq. (20), it is immediate to observe that the right-handed operator captures nonlocality ahead of the point x_0 (in the jth direction), and the left-handed operator is reduced to the classical first-order derivative. From a mathematical standpoint, the definition of the nonlocal operator ensures that, independent of the nature of the kernel, we recover a local behavior every time the size of the nonlocal horizon on any given side of a point approaches (or is equal to) zero. This suggests that the truncation of the nonlocal horizon and the corresponding convolution at the boundary have been accounted for in a consistent manner. From an atomistic or molecular dynamic perspective, the reduction of the left-handed operator to the classical first-order derivative is physically analogous to the annihilation (or removal) of long-range interactions between atoms or molecules close to material boundaries (Tuna et al.,

Before proceeding further, we merely note that the equality $c_{-i}^* =$ c_{+}^{*} holds iff the nonlocal kernel is symmetric and $l_{-} = l_{+}$. The above conditions require that the body has uniform material properties (such that the nonlocal kernel exhibits uniform spatial characteristics) and the point under consideration has a symmetric horizon of nonlocality (possible for points located sufficiently far from the material boundaries).

4. Considerations on thermodynamics

In this section, we explore the implications of a displacement-driven approach on the thermodynamic formulation of the nonlocal solid and we will show how this approach is uniquely equipped to enforce the laws of thermodynamics in a strong (point-wise) sense.

First law of thermodynamics: For a nonlocal solid, the statement of the conservation of energy for a point x includes, in addition to the local strain energy, the energy associated with the long-range interactions with points contained within its horizon of nonlocality. The functional relationship between the energy density (e) and the different energy exchanges (local and nonlocal) is typically expressed as $e = e(\varepsilon_1, \mathcal{R}(\varepsilon_1), \eta)$ where ε_1 is the local strain field, $\mathcal{R}(\varepsilon_1)$ denotes a linear integral operator which models nonlocality in the solid, and η is the entropy of the solid (Polizzotto, 2001). Broadly speaking, the nonlocal

strain in the displacement-driven approach allows combining the local strain ε_1 and its integral $\mathcal{R}(\varepsilon_1)$. More specifically, given the nonlocal kinematic relations described in Section 2, the contribution of the energy contained in the long-range interactions is fully captured in the nonlocal strain. In this context, recall the argument that the nonlocal kinematic relations were a reformulation of the concept of action-at-adistance, and hence carry information of nonlocal interactions within the solid. It immediately follows that the internal energy density of the solid can be expressed explicitly as a function of the nonlocal strain. Mathematically, for the displacement-driven approach, we have $e = e(\varepsilon, \eta)$, where ε is the nonlocal strain. This latter conclusion is remarkable as it allows the first law of thermodynamics to be applied in a strict sense at every point in the domain:

$$\dot{e} = \sigma_{ij} \varepsilon_{ij} + h - q_{i,i} \ \forall \mathbf{x} \in \Omega \tag{21}$$

where the notation (i) indicates the first-order derivative with respect to time, h is the heat generated internally per unit volume, and q is the heat flux density.

Second law of thermodynamics: The second law of thermodynamics states that the internal entropy production rate within a solid is nonnegative for all points inside the solid, that is, $\dot{\eta}_0 \ge 0 \ \forall \ x \in \Omega$. In order to apply the second law of thermodynamics to the displacement-driven formulation, we consider the internal entropy production rate:

$$\dot{\eta}_0 = \dot{\eta} - \left[\frac{h}{T} - \left(\frac{q_i}{T} \right)_i \right] \tag{22}$$

where T denotes the absolute temperature of the solid. In analogy with the classical approach, we introduce the Legendre transformation $\psi = e - T\eta$, where ψ denotes the Helmholtz free energy. By following the rationale presented in defining $e = e(\varepsilon, \eta)$, it immediately follows that $\psi = \psi(\varepsilon, T)$. By using the Legendre transformation along with Eq. (22) we obtain:

$$T\dot{\eta}_0 = \sigma_{ij}\varepsilon_{ij} - \dot{\psi} - \eta \dot{T} - T_{,i}\frac{q_i}{T} \ge 0 \ \forall x \in \Omega$$
 (23)

Note that the statement of the second law of thermodynamics for the displacement-driven approach is analogous to the classical Clausius-Duhem inequality in its function form, hence presenting a clear departure from several classical nonlocal approaches characterized by the presence of additional terms. These additional terms, resulting from a functional dependence of ψ on $\mathcal{R}(\varepsilon_l)$, prevent casting the second law of thermodynamics in a strong-form. Indeed, these terms disappear only when a weak-form is considered (that is, $\int_{\Omega} \dot{\eta}_0 \ge 0$). The ability to satisfy the second law of thermodynamics only in a weak sense is the main source of physical inconsistencies of classical nonlocal formulations, as highlighted in Polizzotto (2001).

The Clausius-Duhem inequality in Eq. (23) can be used to derive thermodynamically consistent constitutive equations which should be equal to the ones introduced in Section 2. By substituting the functional relationship $\psi = \psi(\varepsilon, T)$, the inequality in Eq. (23) is simplified as:

$$T\dot{\eta}_{0} = \left(\sigma_{ij} - \frac{\partial \psi}{\partial \varepsilon_{i,i}}\right)\dot{\varepsilon}_{ij} - \left(\eta + \frac{\partial \psi}{\partial T}\right)\dot{T} - T_{,i}\frac{q_{i}}{T} \ge 0 \ \forall \mathbf{x} \in \Omega$$
 (24)

Since the above inequality must hold for arbitrary choices of the independent fields ε and T at all times, we obtain the following constitutive

$$\sigma_{ij} = \frac{\partial \psi}{\partial \epsilon} \ \forall x \in \Omega \tag{25a}$$

$$\sigma_{ij} = \frac{\partial \psi}{\partial \varepsilon_{ij}} \, \forall \mathbf{x} \in \Omega$$

$$\eta = -\frac{\partial \psi}{\partial T} \, \forall \mathbf{x} \in \Omega$$
(25a)
$$(25b)$$

Finally, by using the above constitutive relations within Eq. (23), we

$$T\dot{\eta}_0 = -T_{,i}\frac{q_i}{T} \ge 0 \ \forall x \in \Omega$$
 (26)

which establishes the strong-form of the second law of thermodynam-

$$\lim_{l_{-j} \to 0} \overline{D}_{x_{j}} \phi = \lim_{l_{-j} \to 0} \left[\frac{D_{x_{j}}^{1} \phi \Big|_{x_{0}}}{2 \int_{x_{0}}^{x_{0_{j}}} \mathcal{K}(\mathbf{x}, \mathbf{x}') d\mathbf{x}'_{j}} \mathcal{K}(\mathbf{x}, \mathbf{x}') d\mathbf{x}'_{j} + c_{+j}^{*} \int_{x_{0_{j}}}^{x_{+j}} \mathcal{K}(\mathbf{x}, \mathbf{x}') D_{x'_{j}}^{1} \phi d\mathbf{x}'_{j}} \right]$$

$$(19)$$

which immediately yields:

$$\lim_{l_{-j}\to 0} \overline{D}_{x_j} \phi = \underbrace{\frac{1}{2} D_{x_j}^1 \phi \Big|_{x_0}}_{\text{Local effect due to truncation of nonlocal horizon}} + c_{+j}^* \int_{x_{0_j}}^{x_{+j}} \mathcal{K}(\mathbf{x}, \mathbf{x}') D_{x_j'}^1 \phi dx_j'$$
Remaining nonlocal interactions

5. Governing equations

In this section, we derive the strong-form of the equilibrium equations governing the response of the nonlocal solid by using variational principles. Note that the governing equations can also be derived by using the more classical Newtonian approach based on force and moment balance over a representative volume element of the nonlocal domain. Although both approaches yield identical results, the variational approach is deemed more direct given that the explicit use of forces and moments balance would require additional care in accounting for the effect of the nonlocal interactions, as described in detail in Polizzotto (2001) and Sidhardh et al. (2021a).

We derive the strong-form of the governing equations by using the Hamilton's principle:

$$\int_{t_1}^{t_2} \delta(\Pi - V - T) dt = 0$$
 (27)

In the above equation, V and T denote the work done by externally applied forces and the kinetic energy of the system, respectively. Recall that Π denotes the total strain energy of the nonlocal solid. Substituting the expressions for the different physical variables, we obtain:

$$\int_{t_1}^{t_2} \delta \left[\underbrace{\frac{1}{2} \int_{\varOmega} (\boldsymbol{\sigma} : \boldsymbol{\varepsilon}) d\mathbb{V}}_{\text{Strain energy}} - \underbrace{\int_{\varOmega} (\overline{\boldsymbol{b}} \cdot \boldsymbol{u}) d\mathbb{V}}_{\text{External work}} - \underbrace{\frac{1}{2} \int_{\varOmega} \rho(\dot{\boldsymbol{u}} \cdot \dot{\boldsymbol{u}}) d\mathbb{V}}_{\text{Kinetic energy}} \right] dt = 0$$

where dV and dA indicate volume and area elements of the nonlocal solid, respectively. \bar{b} and \bar{t} are prescribed values of the body force per

unit volume and the surface traction per unit area, respectively, and ρ denotes the density of the solid. Note that the extended Hamilton's principle in Eq. (27) is a universal statement, in the sense that it is applicable to any nonlocal elasticity formulation, regardless of the definition of the strain energy density and of the nonlocal operator. We merely note that the specific nature of the nonlocal operator (specific to each type of approach) only affects the expression of the governing equations in strong-form and the mathematical simplifications required to derive them. From a physical perspective, the variational statement in Eq. (27) with a nonlocal definition for Π , can be interpreted as the continuum limit of the Hamilton's principle applied to a discrete collection of nonlocal particles with long-range interactions (Silling and Lehoucq, 2010; Dell'Isola et al., 2012, 2015). This is because, the nonlocal definition for the strain energy, can be interpreted as the continuum limit of the sum of the energies corresponding to the long-range interactions between a set of particles that interact in a nonlocal manner (see, for example, continualization of 1D lattices with exponential decay Di Paola et al., 2013 and power-law decay Carpinteri et al., 2014; Patnaik et al., 2021b) in the strength of the long-range interactions).

By simplifying Eq. (28) using principles of variational calculus, we obtain the governing equation as:

$$\widetilde{\nabla} \cdot \sigma + \overline{b} = \rho \ddot{u} \ \forall x \in \Omega \tag{29}$$

The associated boundary conditions are obtained as:

$$\tilde{I}_{\hat{n}} \cdot \sigma = \bar{t} \quad \text{or} \quad u = \bar{u} \quad \forall \ x \in \partial \Omega$$
 (30)

where \bar{u} is the externally applied displacement load. The detailed derivation of the governing equation and the associated boundary conditions (including the variational simplifications and principles associated with the nonlocal operator) is provided in Appendix.

The operator $\tilde{I}_{\hat{n}}(\cdot)$ in Eq. (30) is defined as:

$$\tilde{I}_{\hat{n}}(\cdot) = n_x \tilde{I}_x(\cdot)\hat{x} + n_y \tilde{I}_y(\cdot)\hat{y} + n_z \tilde{I}_z(\cdot)\hat{z}$$
(31)

where $\hat{n} = n_x \hat{x} + n_y \hat{y} + n_z \hat{z}$ is the unit normal vector at the surface of the solid. In the above equation, $\tilde{I}_{x_i}(\cdot)$ is an integral operator defined in the following manner:

$$\tilde{I}_{x_j}\phi = c_{-j}^* \int_{x_j}^{x_j + l_{-j}} \mathcal{K}(\mathbf{x}, \mathbf{x}') \phi dx_j' + c_{+j}^* \int_{x_j - l_{+j}}^{x_j} \mathcal{K}(\mathbf{x}, \mathbf{x}') \phi dx_j'$$
(32)

Further, the gradient operator, denoted by $\widetilde{\boldsymbol{\nabla}}(\cdot)$ in Eq. (29), is a differintegral operator (analogous to $\overline{\nabla}(\cdot)$ in Eq. (6)) containing the above defined integral operators:

$$\widetilde{\nabla}(\cdot) = D_x^1 \left[\widetilde{I}_x(\cdot) \right] \hat{x} + D_y^1 \left[\widetilde{I}_y(\cdot) \right] \hat{y} + D_z^1 \left[\widetilde{I}_z(\cdot) \right] \hat{z} \equiv \widetilde{D}_x(\cdot) \hat{x} + \widetilde{D}_y(\cdot) \hat{y} + \widetilde{D}_z(\cdot) \hat{z}$$
(33)

Note that the natural boundary conditions are integral (and hence, nonlocal) in nature, consistent with existing integral approaches to nonlocal elasticity (Polizzotto, 2001; Romano and Barretta, 2017). From a physical perspective, the nonlocal natural boundary conditions account for the combined effect of long-range forces exerted on the boundary points by points located within the nonlocal solid. While the use of variational principles allowed obtaining the nonlocal natural boundary conditions in a relatively straight-forward manner, the use of global conservation principles (mechanical balance laws) requires a careful modification of the surface tractions to account for the nonlocal interactions of the boundary points. In other terms, Cauchy's postulate for surface tractions requires a modification to account for the nonlocal interactions. This latter aspect has been addressed in detail in Dell'Isola et al. (2012, 2015) and Sidhardh et al. (2021a).

6. Dispersion relations and choice of kernels

The nonlocal elastodynamic framework presented in Section 5 allows for the derivation of wavenumber-frequency dispersion relations describing the transient response of the nonlocal bulk solid. It is anticipated that the dispersion relations functionally depend on the nature of the nonlocal kernel used to model nonlocality within the solid. In this section, we derive the dispersion relations for an unbounded 1D nonlocal isotropic solid and use them to gain insight into the specific effects of the nature of the nonlocal kernel.

The governing equation describing a 1D nonlocal isotropic solid, in the absence of body forces, can be extracted from Eq. (29) by assuming $u \equiv u\hat{x}$ (as commonly done in literature) and $\bar{b} = 0$, as:

$$E\widetilde{D}_{x}\overline{D}_{x}u = \rho \ddot{u} \tag{34}$$

where E is the modulus of elasticity of the isotropic solid. To obtain the dispersion relation, we substitute in the elastodynamic equation the following ansatz:

$$u(x,t) = u_0 e^{i(kx - \omega t)} \tag{35}$$

where u_0 is the amplitude of the longitudinal wave, k denotes the wave-number, ω denotes the angular frequency of free longitudinal vibrations, and $i = \sqrt{-1}$. Using the expressions for the differ-integral operators in Eq. (34), we obtain the following expression for the dispersion relation in an unbounded nonlocal solid:

$$\omega^{2} + ike^{-ikx} \frac{E}{\rho} D_{x}^{1} \left[\int_{-\infty}^{\infty} \mathcal{K}(x, x') \int_{-\infty}^{\infty} \mathcal{K}(x', s') e^{iks'} ds' dx' \right] = 0$$
 (36)

The above expression provides important insights into the nature of the formulation. First, the expression suggests that for a well-posed formulation resulting in bounded wave speeds, it is essential that the convolution integrals in Eq. (36) exist and are bounded. This latter condition is always satisfied if the nonlocal kernel: (1) decays spatially with the increasing inter-particle distance, that is, $D^1_{x-x'}\mathcal{K}(x,x') < 0 \ \forall \{x,x'\}$, and (2) is positive-definite (more concretely, the Fourier transform of the kernel is positive everywhere Bažant and Chang, 1984). Note also that, a decaying kernel, also guarantees the existence of the integrals in Eq. (14) which are essential to enable a frame-invariant formulation. This condition is also consistent with existing approaches to nonlocal elasticity, which invariably use decaying kernels (Eringen and Edelen, 1972; Silling, 2000; Lazopoulos, 2006). At this stage, following the analysis of frame-invariance and of the dispersion relations, we are well-equipped to summarize all the sufficient requirements for the nonlocal kernel in order to ensure a physically consistent formulation: the kernel should be positive-definite and must decay monotonically with increase in the interparticle distance.

Note that further simplifications of the expression in Eq. (36) requires the specific functional definition of the nonlocal kernel. From a practical perspective, this suggests that the applicability of a given functional form of the nonlocal kernel, to model a certain class of nonlocal structures, depends on whether the dispersion characteristics obtained by simplification of Eq. (36) match experimentally obtained dispersion characteristics of the class of materials under consideration. This latter aspect becomes evident by considering the example of the exponential and the power-law kernels introduced in Section 2. The dispersion relations for the exponential and the power-law kernels are obtained by using Eq. (36) as:

Exponential kernel:
$$\left(\frac{\omega}{k}\right)^2 = \frac{E}{\rho} \left(\frac{1}{1+k^2 l_0^2}\right)^2$$
 (37a)

Power-law kernel: $\left(\frac{\omega}{k}\right)^2 = \frac{E}{\rho} \left[\cos\left(\pi + \alpha\pi\right) + i \sin\left(\pi + \alpha\pi\right)\right] \left(kl^*\right)^{2(\alpha-1)}$

Attenuation (37b)

While the derivation of the dispersion relation is straightforward for the exponential kernel (given the exponential nature of both the kernel and the assumed wave solution), some special relations are required to derive the dispersion relations for the power-law kernel. These relations (that concern the fractional-order derivatives of an exponential function) as well as the derivation of the dispersion relations for the power-law kernel can be found in Patnaik et al. (2021b). In the power-law dispersion, $l^* = 1$ m is a dimensional constant which is used to enforce dimensional consistency for the 1D unbounded solid (Hollkamp

et al., 2019; Patnaik et al., 2021b). This constant is required for the 1D unbounded solid because frame-invariance is trivially satisfied for the only possible rigid-body motion, that is, translation in this case (Patnaik et al., 2021b).

The nature of the dispersion relations obtained for the exponential and power-law kernels presented above lead to the following observations and conclusions:

- The use of an exponential kernel is suitable for modeling nonlocal structures which are dispersive but not attenuating in nature. Examples of such structures can include micro- and nano-structures such as carbon nanotubes, thin films, monolayer graphene sheets, and nanobeams made of metals (Eringen, 1972; Pradhan and Murmu, 2009; Wang et al., 2011; Askes and Aifantis, 2011; Lim et al., 2015). Additionally, macrostructures made of functionally graded materials and sandwiched cores, also exhibit similar dispersive characteristics (Romanoff and Reddy, 2014; Romanoff et al., 2020).
- The power-law kernel is suitable for materials which exhibit anomalous attenuation and dispersion. Note that the real and imaginary parts of the dispersion relation in Eq. (37b) correspond to the propagating and attenuating component of the wave. Examples of such structures can include macrostructures such as highly scattering media (e.g. fractal, porous, and layered media) (Fellah et al., 2004a; Buonocore et al., 2019; Patnaik et al., 2021a) and even animal tissues (Fellah et al., 2004b; Magin, 2010). Periodic media (Hollkamp et al., 2019; Hollkamp and Semperlotti, 2020; Patnaik and Semperlotti, 2020a) and structures with intentionally designed nonlocal geometric features (such as, for example, acoustic black hole metamaterials Nair, 2019 and metasurfaces with intentionally designed nonlocality Zhu et al., 2020) also exhibit similar characteristics. Remarkably, the dispersion as well as the attenuation in the wave speeds in several classes of these structures, exhibit a power-law dependence on the wave-number as also captured by the use of the power-law kernel (Fellah et al., 2004b; Hollkamp and Semperlotti, 2020; Fellah et al., 2004a; Buonocore et al., 2019; Patnaik and Semperlotti, 2020a).
- The dispersion characteristics obtained using the exponential kernel matches exactly the dispersion relation obtained via classical differential models recovered from Eringen's approach by using exponential kernels (Askes and Aifantis, 2011; Wang et al., 2011). The motivation behind adopting the differential model follows from a good match of the predicted dispersion against experimental observations, particularly for different nanostructures such as, for example, graphene tubules and carbon nanotubes. As established in (Romano et al., 2017), this procedure of obtaining a simplified differential model (based on the strain-driven approach) leads to ill-posed formulations with inconsistent predictions for different static loading conditions. On the contrary, the displacement-driven approach enables a well-posed static framework while recovering the same dynamic characteristics.
- Since the differential approaches to nonlocal elasticity are recovered by assuming (only) the exponential kernel within Eringen's approach (Pradhan and Murmu, 2009; Wang et al., 2011; Askes and Aifantis, 2011; Lal and Dangi, 2019), these approaches are not suitable to model structures which exhibit anomalous attenuation-dispersion characteristics. This observation suggests that the displacement-driven approach is more general, since the kernel can be modified to capture the behavior of a wider class of size-dependent structures.

The above discussion highlights the relevance of the generalized procedure, involving analysis of both singular (e.g. power-law) and non-singular (e.g. exponential) kernels, adopted in this study. The discussion also suggests that the application of any nonlocal approach to modeling of practical structures must involve the *a priori* selection

of a suitable kernel, guided by experimentally observed dispersion characteristics.

7. Application to nonlocal beams and plates

In this section, we use the displacement-driven approach to analyze the static response of slender nonlocal structures, including a Timoshenko beam and a Mindlin plate. Similar to previous analyses, we will consider separately the effect of either the exponential or the powerlaw kernel, on the static response of the nonlocal structures subject to different loading conditions. For each structure, we will first present the nonlocal constitutive formulation, followed by the numerical results generated using the fractional-order finite element method (f-FEM). The f-FEM is a highly general formulation that is well-suited for both singular and non-singular kernels (Patnaik et al., 2020b). The algorithm of the f-FEM is discussed in detail in (Patnaik et al., 2021c) and, for the sake of brevity, details are not repeated here. For completeness, we note that the nonlocal formulation involving the exponential kernel can also be simulated by adapting the classical nonlocal finite element procedure (Polizzotto, 2001; Ansari et al., 2018; Sidhardh and Ray, 2018), from a strain-driven approach to a displacement-driven approach. Since we have considered shear-deformable structures in the following analyses, we adopted a reduced-order Gauss quadrature integration for the evaluation of the shear stiffness matrices in order to avoid shear-locking effects (Reddy, 2003). More specifically, for the nonlocal Timoshenko beam we used 2 and 1 Gauss quadrature elements to numerically integrate the bending and shear stiffness matrices, respectively. Analogously, for the nonlocal Mindlin plate, we used 2×2 and 1×1 Gauss quadrature points for the bending and shear stiffness matrices, respectively.

Analogous to classical finite element procedures, the numerical solution in the f-FEM is obtained by discretization of the Hamiltonian of the nonlocal structure by using an isoparametric formulation. Consequently, we only provide the weak-form of the governing equations for both the nonlocal Timoshenko beam and the nonlocal Mindlin plate. The corresponding strong-form of the governing equations can be easily obtained by following the derivation of the 3D governing equations in Section 5. In fact, the strong-form nonlocal governing equations do not generally admit closed-from analytical expressions for the most general loading conditions. Hence, for the sake of brevity, we do not provide again the strong-form of the governing equations.

7.1. Application to nonlocal beams

In this section, we apply the displacement-driven approach to model and analyze the static response of nonlocal shear-deformable beams. We consider a nonlocal beam of uniform cross-section with length L_b , width b_b and thickness h_b . A schematic of the beam, along with the chosen Cartesian coordinate axes, is provided in Fig. 2. As evident from Fig. 2, the coordinate axes are chosen such that the mid-plane of the beam is identified as z=0. The displacement field components at a spatial point x(x,y,z) of the beam can be expressed by following the shear-deformable Timoshenko formulation as Reddy (2003):

$$u(\mathbf{x}) = u_0(x) - z\theta_x(x) \tag{38a}$$

$$w(\mathbf{x}) = w_0(\mathbf{x}) \tag{38b}$$

where u_0 and w_0 denote the axial and the transverse displacement of the mid-plane of the beam, respectively. θ_x denotes the rotation of the normal to the mid-plane of the beam, about the \hat{x} axis.

Employing the nonlocal strain–displacement relation given in Eq. (4a), we obtain the following expressions for the strains developed in the nonlocal beam:

$$\varepsilon_{xx}(\mathbf{x}) = \overline{D}_x u_0(x) - z \overline{D}_x \theta_x(x) \tag{39a}$$

$$\gamma_{xz}(\mathbf{x}) = \overline{D}_x w_0(x) - \theta_x(x) \tag{39b}$$

The stress developed in the beam can be derived from the stress–strain constitutive relation in Eq. (4b).

Using the nonlocal strains and stresses generated in the beam, the total strain energy can be expressed as:

$$\Pi = \frac{1}{2} \int_0^{L_b} \int_{-\frac{b_b}{2}}^{\frac{b_b}{2}} \int_{-\frac{b_b}{2}}^{\frac{b_b}{2}} \left[\sigma_{xx} \epsilon_{xx} + \kappa_s \sigma_{xz} \gamma_{xz} \right] dz dy dx \tag{40}$$

where κ_s is the shear correction factor chosen as $\kappa_s = 5/6$ throughout this study (Reddy, 2003). Finally the work done by external loads on the beam can be expressed as:

$$V = \int_{0}^{L_{b}} \int_{-\frac{b_{b}}{2}}^{\frac{b_{b}}{2}} \int_{-\frac{h_{b}}{2}}^{\frac{h_{b}}{2}} \left[F_{x} u_{0} + F_{z} w_{0} + M_{\theta_{x}} \theta_{x} \right] dz dy dx \tag{41}$$

where $\{F_x, F_z\}$ are the loads applied externally in the \hat{x} and \hat{z} directions, respectively. Further, M_{θ_x} is the moment applied about the \hat{y} axis. The nonlocal equilibrium equations describing the static response of the nonlocal beam can now be derived by applying variational principles $(\delta(\Pi-V)=0)$.

7.1.1. Results and discussion

In this section, we analyze the effect of different kernels and different loading conditions on the static bending response of the nonlocal beam. In all simulations, we considered an isotropic beam having Young's modulus $E=30~\mathrm{GPa}$ and Poisson's ratio v=0.3. The geometric dimensions of the beam were taken as $L_b=1\mathrm{m}$ and $b_b=h_b=L_b/10$. As mentioned previously, we analyzed the effect of two different kernels: the exponential kernel and the power-law kernel, on the response of the nonlocal beam. In each case, we have assumed an isotropic and symmetric horizon of nonlocality such that $l_{-x}=l_{+x}=l_f$, for points sufficiently far from the boundaries. Recall from Sections 2 and 3 that this symmetry is broken $(l_{-x}\neq l_{+x})$ for points close to the boundaries (see Fig. 1). Note that while the choice of the different material properties and geometric parameters was somewhat arbitrary, their numerical values do not affect the applicability of the model and the generality of the results presented here below.

Using the above described scheme, we analyzed two different loading conditions: (a) a cantilever beam subject to a transverse force at its end-point, and (b) a simply-supported beam subject to a uniformly distributed transverse load (UDTL). For each boundary condition, we obtained the response of the beam for the following different kernel parameters:

- Exponential kernel: the kernel parameter l_0 was varied in (0,0.005] m (= $(0,L_b/200]$) and the nonlocal horizon parameter l_f was varied in [0.5,1]m (= $[L_b/2,L_b]$). The lowest value for l_0 was chosen as $l_0=10^{-6}$ instead of zero because the choice of $l_0=0$ leads to a singularity within the exponential kernel, wherein the exponential kernel reduces to a Dirac-delta operator (Romano et al., 2017).
- *Power-law kernel*: the nonlocal horizon l_f was varied in [0.5,1]m (= $[L_b/2,L_b]$) and the kernel parameter α , also called as the fractional-order (Patnaik and Semperlotti, 2020a), was varied in [0.7,1].

The numerical results, expressed in terms of the maximum transverse displacement of the beam, are presented in Figs. 3 and 4 for the exponential kernel and the power-law kernel, respectively. Note that the maximum transverse displacement of the nonlocal beam is non-dimensionalized against the analogous value obtained for a local beam. The non-dimensionalized maximum transverse displacement is indicated by \overline{w} . Results show that the proposed displacement-driven approach predicts a consistent softening response, that is, $\overline{w} > 1$, for different combinations of the kernel parameters and loading conditions.

Fig. 2. Schematic of the rectangular beam illustrating the different geometric parameters.

Given this general observation, we proceed to critically analyze the effects of the two different kernels and of their parameters.

The results presented for the exponential kernel in Fig. 3, lead to the following observations:

• Effect of l_0 : In the limiting case $l_0 \rightarrow 0$, the classical (local) solution $\overline{w} \rightarrow 1$ is recovered (Romano and Barretta, 2017; Pisano et al., 2021). This observation is consistent with the fact that $l_0=0$ reduces the exponential kernel to the Dirac-delta operator, which results in a reduction of the nonlocal model to its local elastic counterpart. Note also that, an increase in the value of l_0 first leads to an increase in the degree of softening followed by an asymptotic decline, as a function of l_0 . Nonetheless, irrespective of the specific value of l_0 , the nonlocal beam exhibits a softening effect, that is, $\overline{w} > 1$. This behavior is observed independently of the loading conditions and is a direct result of the nature of the exponential kernel as discussed in the following.

Note that the strength of the nonlocal interactions between two material points, separated by a certain distance (say d_0) within the nonlocal beam, is directly related to the value of the nonlocal kernel. In this case, the strength of the nonlocal interactions can be given as $\propto [\exp(-d/l_0)]/l_0$ (the l_0 in the denominator appears from the multipliers c_{-x}^* and c_{+x}^*). Consider the following function for a fixed value of d_0 :

$$g(l_0) = \frac{1}{l_0} \exp\left(-\frac{d_0}{l_0}\right) \tag{42}$$

A quick analysis of the above function reveals that $g(l_0)$ increases initially with an increase in l_0 , to reach a global maximum at $l_0=d_0$. Following the maximum, it asymptotically approaches zero with increase in l_0 , that is, $\lim_{l_0\to\infty}g(l_0)=0$. It is exactly this behavior that is reflected in the static response curves of the nonlocal beam in Fig. 3. Notably, this behavior is also observed in the response of atomic lattice models (Eringen, 1983; Lim et al., 2015; Pisano et al., 2021). This observation is also consistent with our discussion in Section 6, where we indicated that the dispersion relation obtained from the exponential kernel is well suited to model the dynamic response of nano- and microstructures, typically presented in the form of atomic lattice chains. Further, the result presented above is also consistent with predictions made for nonlocal beams in recently developed well-posed integral approaches (Pisano et al., 2021).

• Effect of I_f : It appears that the length of the horizon of nonlocality l_f does not significantly affect the degree of softening when $\mathcal{O}(l_f/L_b)=1$. Recall that the parameter l_f physically represents the size of the horizon of nonlocality, that is, it determines the distance beyond which two particles no longer interact via longrange forces. In this context, the apparent insensitivity of \overline{w} to changes in l_f (in the chosen range) is a direct result of the fact that $\mathcal{K}(x,x')=e^{-|x-x'|/l_0}\approx 0$ for $|x-x'|>5l_0$. Thus, the effect of the nonlocal kernel is always accounted completely (in the chosen range for l_f) and does not change appreciably with a further increase in l_f . However, note from Section 3 that, l_f plays a critical role (along with c_{-x}^* and c_{+x}^*) in achieving frame-invariance, dimensional consistency, as well as completeness of the kernel.

We now proceed to analyze the results obtained for the nonlocal beam modeled via the power-law kernel. A detailed analysis of the results presented in Fig. 4 leads to the following conclusions:

- *Effect of* α : For $\alpha = 1$ we recover the classical (local) solution $\overline{w} = 1$ 1, consistent with the nature of the power-law kernel (Patnaik and Semperlotti, 2020a; Sumelka, 2014). Next, observe that a decrease in the value of α leads to a consistent increase in the degree of softening, irrespective of the nature of the loading conditions. A decrease in the value of α leads to an increase in the value of the power-law kernel $|x - x'|^{-\alpha}$ for a fixed value of |x-x'|. This suggests that a decrease in the value of α leads to an increase in the degree of nonlocality and a higher degree of softening. We merely note that the above findings are also consistent with results presented in existing fractional-order approaches to nonlocal elasticity (which employ the power-law kernel) (Patnaik et al., 2020b, 2021c). We highlight that there exists a critical value of α (= 0.4 for the nonlocal beam), below which the beam undergoes excessive softening and the model breaks down. More detailed discussions on this aspect can be found in Patnaik et al. (2020b), Sidhardh et al. (2020) and Sumelka (2014).
- Effect of l_f : An increase in the value of l_f leads to significant softening in the case of a power-law kernel. The enhanced softening is a direct result of the fact that, an increase in the value of l_f leads to an increase in the size of the horizon of nonlocality. Consequently, a larger number of points within the solid contribute to the nonlocal interactions leading to an increase in the degree of nonlocality. Again, this observation is supported by results presented in fractional-order approaches to nonlocal elasticity (Patnaik et al., 2020b, 2021c). Note that, unlike constraints on the lower limit for α , the value of l_f can approach zero. In fact, in the limiting case $l_f \rightarrow 0$, we recover the classical local solution (Sidhardh et al., 2021a; Patnaik et al., 2021b).

7.2. Application to nonlocal plates

We conclude this study by analyzing the response of nonlocal shear-deformable plates, in a manner similar to the analysis of nonlocal beams in Section 7.1. For this purpose, we consider a rectangular plate of uniform thickness, illustrated in Fig. 5. The length, width, and thickness of the plate are denoted by L_p , B_p and h_p , respectively. The Cartesian reference frame, as indicated in Fig. 5, is chosen such that z=0 denotes the mid-plane of the plate. In the chosen reference frame, the displacement field components at a spatial point x(x,y,z) can be expressed by following the shear-deformable Mindlin formulation as Reddy (2003):

$$u(\mathbf{x}) = u_0(x, y) - z\theta_x(x, y) \tag{43a}$$

$$v(\mathbf{x}) = v_0(x, y) - z\theta_v(x, y) \tag{43b}$$

$$w(\mathbf{x}) = w_0(\mathbf{x}, \mathbf{y}) \tag{43c}$$

where u_0 , v_0 , and w_0 denote the displacements at the mid-plane of the plate along the \hat{x} , \hat{y} , and \hat{z} directions. θ_x and θ_y denote the rotations of the transverse normal at the mid-plane of the plate, about the \hat{y} and \hat{x} axes.

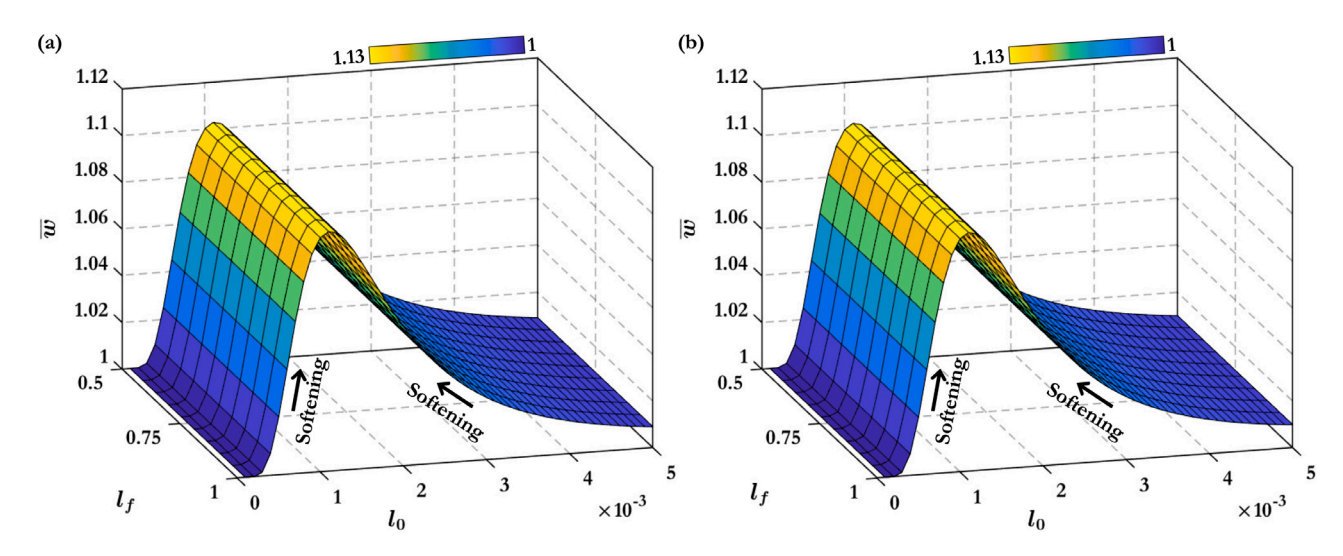


Fig. 3. Bending response measured in terms of the maximum non-dimensionalized displacement of the nonlocal beam, modeled using the exponential kernel. The beam is (a) a cantilever beam subject to an transverse load at its end-point, and (b) simply-supported at all its edges and subject to a UDTL. The response is parameterized for different values of the kernel parameter I_0 and the nonlocal horizon I_f .

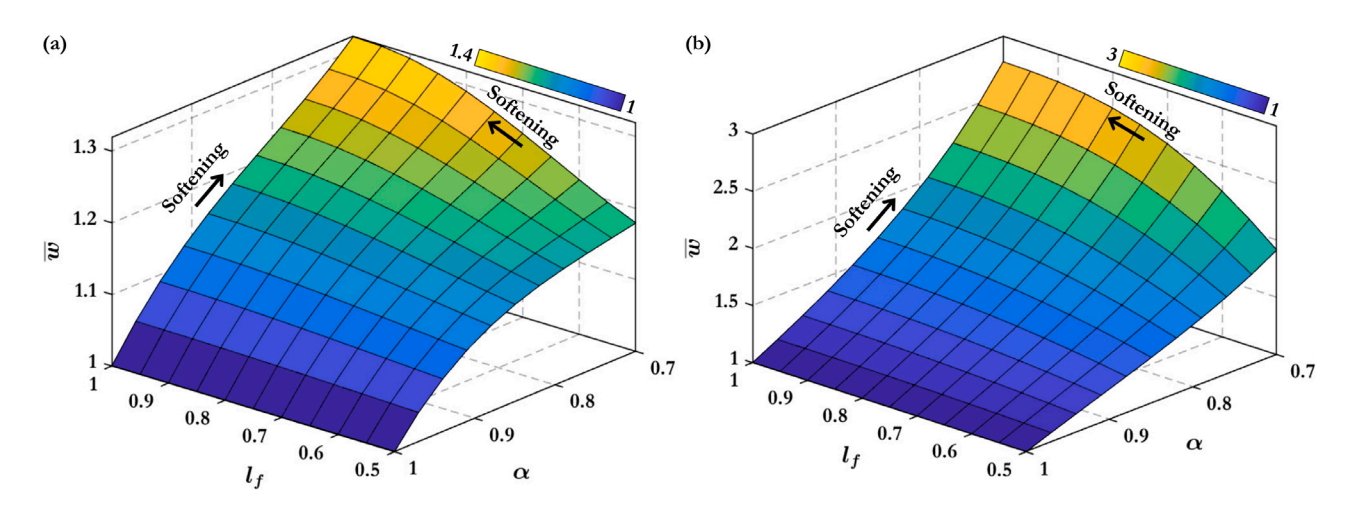
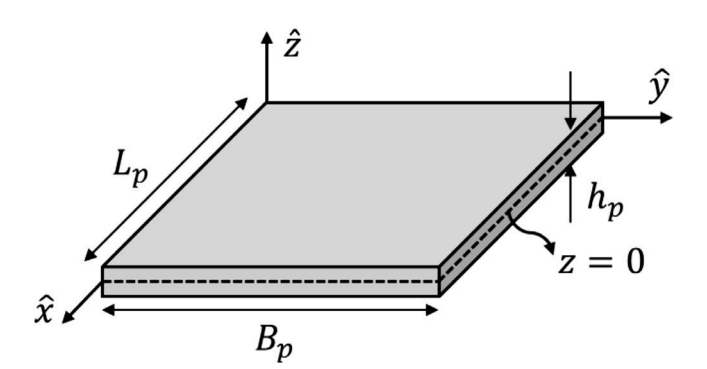


Fig. 4. Bending response measured in terms of the maximum non-dimensionalized displacement of the nonlocal beam, modeled using the power-law kernel. The beam is (a) a cantilever beam subject to an transverse load at its end-point, and (b) simply-supported at all its edges and subject to a UDTL. The response is parameterized for different values of the kernel parameter α and the nonlocal horizon l_f .



 $\textbf{Fig. 5.} \ \ \textbf{Schematic} \ \ \ \textbf{of the rectangular} \ \ \ \textbf{plate} \ \ \ \textbf{illustrating} \ \ \textbf{the different geometric} \\ \textbf{parameters.} \\$

The nonzero nonlocal strains, corresponding to the deformation field in Eq. (43), are obtained by using Eq. (4a) as:

$$\varepsilon_{xx}(\mathbf{x}) = \overline{D}_x u_0(x, y) - z \overline{D}_x \theta_x(x, y) \tag{44a}$$

$$\varepsilon_{yy}(\mathbf{x}) = \overline{D}_y v_0(x, y) - z \overline{D}_y \theta_y(x, y) \tag{44b}$$

$$\gamma_{xy}(\mathbf{x}) = \overline{D}_y u_0(x, y) + \overline{D}_x v_0(x, y) - z \left[\overline{D}_y \theta_x(x, y) + \overline{D}_x \theta_y(x, y) \right]$$
(44c)

$$\gamma_{xz}(\mathbf{x}) = \overline{D}_x w_0(x, y) - \theta_x(x, y) \tag{44d}$$

$$\gamma_{vz}(\mathbf{x}) = \overline{D}_v w_0(x, y) - \theta_v(x, y) \tag{44e}$$

The nonlocal stresses developed in the nonlocal plate can now be evaluated using the stress–strain constitutive relation in Eq. (4b).

Using the nonlocal strains and stresses generated in the plate, the total strain energy can be expressed as:

$$\Pi = \frac{1}{2} \int_{0}^{L_{p}} \int_{0}^{B_{p}} \int_{-\frac{h_{p}}{2}}^{\frac{h_{p}}{2}} \left[\sigma_{xx} \varepsilon_{xx} + \sigma_{yy} \varepsilon_{yy} + \sigma_{xy} \gamma_{xy} + \kappa_{s} \sigma_{xz} \gamma_{xz} \right. \\
\left. + \kappa_{s} \sigma_{yz} \gamma_{yz} \right] dz dy dx \tag{45}$$

Finally the work done by external loads on the plate can be expressed as:

$$V = \int_0^{L_p} \int_0^{B_p} \int_{-\frac{h_p}{2}}^{\frac{h_p}{2}} \left[F_x u_0 + F_y v_0 + F_z w_0 + M_{\theta_x} \theta_x + M_{\theta_y} \theta_y \right] dz dy dx$$
(46)

where $\{F_x, F_y, F_z\}$ are the loads applied externally in the \hat{x} , \hat{y} , and \hat{z} directions, respectively. Further, $\{M_{\theta_x}, M_{\theta_y}\}$ are the moments applied about the \hat{y} and \hat{x} axes, respectively. The nonlocal equilibrium differential equations describing the static response of the nonlocal plate can now be derived by applying variational principles. The response of the nonlocal plate is numerically simulated using the f-FEM and the results are presented in the following section.

7.2.1. Results and discussion

In this section, we analyze the effect of different kernels and different boundary conditions on the static bending response of the nonlocal plate. In all the simulations, we considered an isotropic plate with material properties identical to the nonlocal beam in Section 7.1.1. The in-plane dimensions of the plate were chosen as $L_n = B_n = 1$ m, and thickness was chosen as $h_p = L_p/10$. We considered the effect of the exponential kernel and the power-law kernel, similar to the analysis conducted for the nonlocal beam. In each case, we have assumed an isotropic and symmetric horizon of nonlocality such that $l_{-1} = l_{+1} = l_f$, for points sufficiently far from the boundaries. We analyzed the static response of the plate subject to a UDTL for two different kinds of boundary conditions: (a) the plate clamped at all the edges, and (b) the plate simply-supported at all its edges, for different combinations of the kernel parameters. The constraints on the generalized displacement coordinates corresponding to these boundary conditions are as follows Reddy (2003):

$$\begin{array}{l} \text{Clamped plate} : \left\{ \begin{array}{c} \hat{x} = \{0, L_p\} : u_0 = v_0 = w_0 = \theta_x = \theta_y = 0 \\ \hat{y} = \{0, B_p\} : u_0 = v_0 = w_0 = \theta_x = \theta_y = 0 \end{array} \right. \\ \text{Simply-supported plate} : \left\{ \begin{array}{c} \hat{x} = \{0, L_p\} : v_0 = w_0 = \theta_y = 0 \\ \hat{y} = \{0, B_p\} : u_0 = w_0 = \theta_x = 0 \end{array} \right. \end{aligned} \tag{47a}$$

For each boundary condition, we obtained the response of the plate for the following different kernel parameters:

- Exponential kernel: the kernel parameter l_0 was varied in (0,0.005]m (= $(0,L_p/200]$) and the nonlocal horizon parameter l_f was varied in [0.5,1]m (= $[L_p/2,L_p]$). As for the beam, the lowest value for l_0 was chosen as $l_0=10^{-6}$ instead of zero.
- *Power-law kernel*: the nonlocal horizon parameter l_f was varied in [0.5,1]m (= $[L_p/2,L_p]$) and the kernel parameter α was varied in [0.7,1]. Similar to the nonlocal beam, there exists a constraint on the lower limit of α (=0.4 for the nonlocal plate), while the value of l_f can approach to zero (Patnaik et al., 2021c).

The numerical results, in terms of the maximum transverse displacement obtained at the mid-point of the plate, are presented in Figs. 6 and 7 for the exponential kernel and the power-law kernel, respectively. Analogous to the nonlocal beam, the transverse displacement of the mid-point of the nonlocal plate is non-dimensionalized against the analogous value obtained for a local Mindlin plate. As evident from the results, the considerations noted for the nonlocal Timoshenko beam directly extend to the nonlocal Mindlin plate as well.

7.3. Few additional remarks

The displacement-driven approach predicts a consistent softening response for both nonlocal beams and plates, irrespective of the nature of the kernel and the loading conditions. This is a significant outcome when compared to the often incoherent predictions of classical (integer-order) strain-driven integral approaches (Challamel and

Wang, 2008; Fernández-Sáez et al., 2016; Romano et al., 2017). The results obtained from the displacement-driven approach are free from stiffening effects or even the absence of nonlocal effects noted in some strain-driven methods, under selected loading conditions. This latter statement does not suggest that stiffening effects are not expected in nonlocal structures; it only implies that stiffening effects should not be predicted by strain-driven approaches (Romano et al., 2017; Pisano et al., 2021). Indeed, several nonlocal structures do exhibit stiffening effects (Romano et al., 2017; Patnaik et al., 2021b; Pisano et al., 2021). In this context, we highlight here that the displacementdriven approach can be extended in a straight-forward and physically consistent manner to capture both stiffening and softening effects. This has been established exclusively for the power-law kernel in Patnaik et al. (2021b). Further, the displacement-driven approach is also wellsuited for the geometrically nonlinear analyses of nonlocal structures. The extension to geometrically nonlinear analyses has been performed in Sidhardh et al. (2020, 2021b) and Patnaik et al. (2020c) to analyze the nonlinear bending and postbuckling response of nonlocal structures described by the power-law kernel.

In addition to the above discussed capabilities, the displacement-driven approach also enables a direct route to modeling physical phenomena involving discontinuities (such as, for example, fracture and impact). In order to demonstrate the latter ability, we present here below, some connections of the displacement-driven approach with peridynamics (Silling, 2000; Silling and Lehoucq, 2010). However, we will also discuss towards the end of this section, that there are some important and notable differences between the peridynamic approach and the displacement-driven approach.

The key characteristic of the peridynamic approach consists in the purely *integral nature* of the formulation (a direct result of the purely integral nature of peridynamic nonlocal operator) which allows the resulting formulation to model structural damage, fracture, and other discontinuities in a straightforward fashion (Silling, 2000). In this regard, the nonlocal operator used in the displacement-driven approach (defined in Eq. (6)) can be expressed in a purely integral form, analogous to the peridynamic nonlocal operator, following a few mathematical manipulations outlined below. First, the definition of the nonlocal operator in Eq. (6) is recast as:

$$\overline{D}_{x_j} \phi = \int_{\overline{\Omega}_i} c_i^* \mathcal{K}(\mathbf{x}, \mathbf{x}') \left[D_{x_j'}^1 \left(\phi(x_j') - \phi(x_j) \right) \right] dx_j'$$
(48)

where ϕ is an arbitrary function. Note that $\phi(x_j)$ in the previous equation is independent of x_j' which allows us to bring the same term within $D_{x_j'}^1(\cdot)$. Next, by using integration-by-parts, we obtain that:

$$\overline{D}_{x_{j}}\phi = \int_{\overline{\Omega}_{j}} c_{j}^{*} \left[D_{x'_{j}}^{1} \mathcal{K}(\mathbf{x}, \mathbf{x}') \right] \left[\phi(x_{j}) - \phi(x'_{j}) \right] dx'_{j}$$

$$+ c_{j}^{*} \left[\mathcal{K}(\mathbf{x}, \mathbf{x}') \left(\phi(x'_{j}) - \phi(x_{j}) \right) \right] \Big|_{x_{-j}}^{x_{+j}}$$

$$\phi_{0}$$

$$(49)$$

where, recall that, $\{x_{-_j}, x_{+_j}\}$ denote the terminals of the horizon of nonlocality $\overline{\Omega}_i$. Eq. (49) can be expressed finally as:

$$\overline{D}_{x_j} \phi = \underbrace{\int_{\overline{\Omega}_j} c_j^* \overline{\mathcal{K}}(\mathbf{x}, \mathbf{x}') \left[\phi(x_j) - \phi(x_j') \right] dx_j'}_{\overline{\mathfrak{D}}_{x_j} \phi - \phi_0} + \phi_0$$
(50)

where we assumed that the constant of integration ϕ_0 is absorbed within the modified nonlocal operator (that is, $\overline{\mathfrak{D}}_{x_j}\phi$). Further, in obtaining Eq. (50) from Eq. (49), we denoted $D^1_{x_j'}\mathcal{K}(\mathbf{x},\mathbf{x}')=\overline{\mathcal{K}}(\mathbf{x},\mathbf{x}')$.

The following additional remarks are essential to put the above analysis in perspective:

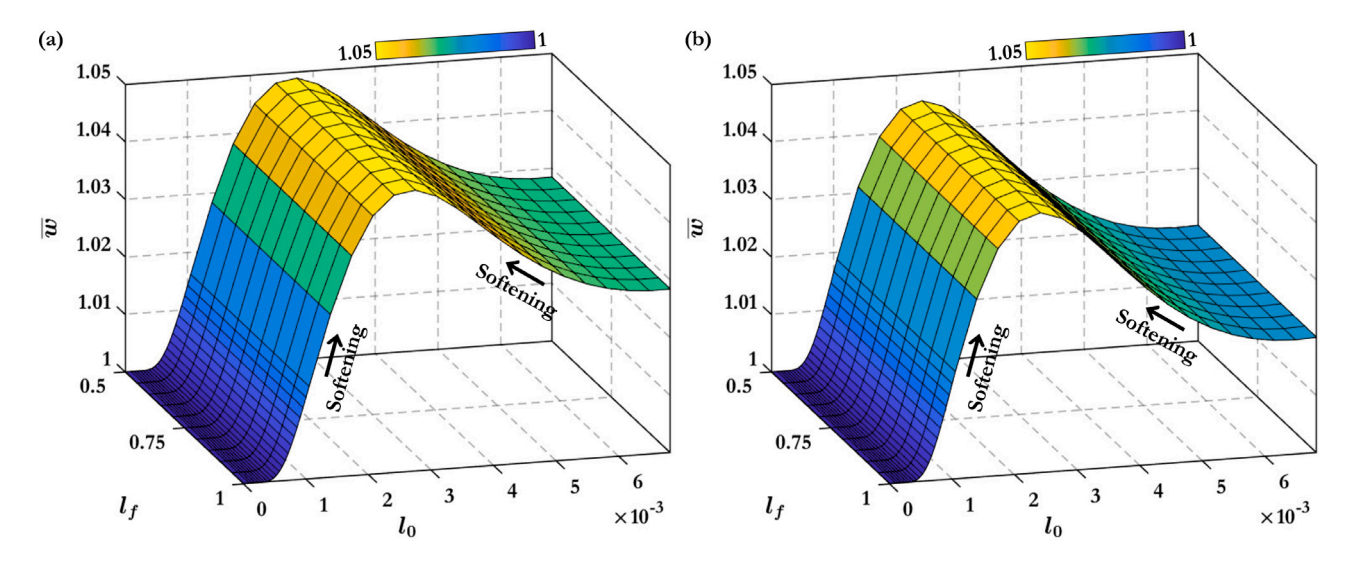


Fig. 6. Bending response measured in terms of the non-dimensionalized displacement at the center point of the nonlocal plate subject to a UDTL and modeled using the exponential kernel. The plate is (a) clamped at all its edges and (b) simply-supported at all its edges. The response is parameterized for different values of the kernel parameter I_0 and the nonlocal horizon I_f .

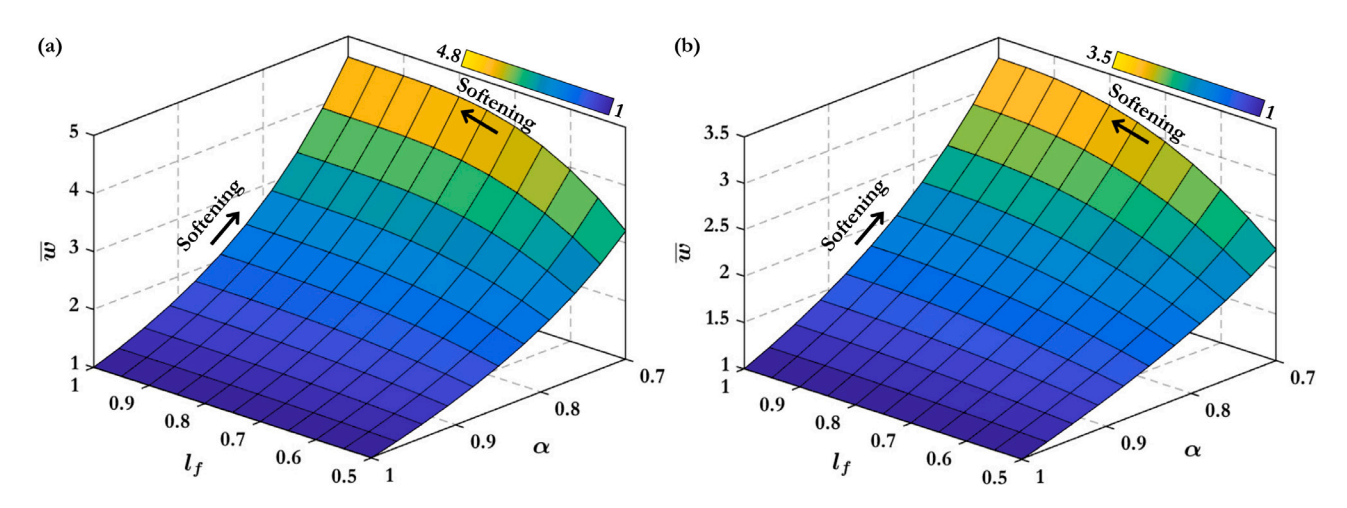


Fig. 7. Bending response measured in terms of the non-dimensionalized displacement at the center point of the nonlocal plate subject to a UDTL and modeled using the power-law kernel. The plate is (a) clamped at all its edges and (b) simply-supported at all its edges. The response is parameterized for different values of the kernel parameter α and the nonlocal horizon I_f .

- Note that the functional expression for the modified nonlocal operator in Eq. (50), in principle, matches the functional expression of the peridynamic nonlocal operator (Silling, 2000). More specifically, analogous to the peridynamic nonlocal operator, the direct dependence of the nonlocal operator on the displacement field rather than its spatial derivatives, enables the resulting formulation to capture structural discontinuities efficiently. This latter characteristic of the displacement-driven approach is in direct contrast with the classical strain- or stress-driven approaches to nonlocal elasticity which, as discussed in Silling and Lehoucq (2010), are not amenable to the modeling of phenomena involving discontinuities.
- While, following the above discussion, it might appear that the displacement-driven approach is closely related to the peridynamic approach, there are important differences to be considered, owing to the fundamental differ-integral nature of the displacement-driven approach (as opposed to the purely integral nature of the peridynamic approach). A direct result of this difference is evident from the nature of the constant of integration φ₀ that appears from the boundary of the nonlocal horizon (see Eq. (49)) in the displacement-driven approach and is absent in the

peridynamic approach. Hence, in order to achieve *true equivalence* between both the approaches it is required that $\phi_0 \to 0$. This latter condition is possible only when the nonlocal kernel approaches $\mathcal{K}(x,x')\to 0$ at the ends of the nonlocal horizon $(\{x_{-j},x_{+j}\})$ in all the directions. While this latter condition is not guaranteed for all kernels, the discussion on the ability of the displacement-driven approach in capturing discontinuities still holds true.

There exists yet another perspective on the nature of the term ϕ_0 . Note that this term can in principle be treated as a jump parameter that enables to capture discontinuous phenomena such as, for example, flow across dissimilar interfaces, evolution of microstructure due to nucleation of dissimilar grains, or even dynamic fracture. In fact, this concept appears analogous to the formalism used in Patnaik and Semperlotti (2021d), where a unique mathematical operator available from the mathematical field of variable-order calculus was utilized to design a similar jump parameter to simulate dynamic fracture.

• In addition to the nature of the term ϕ_0 , a major difference between the peridynamic approach and the displacement-driven approach follows from the route followed to achieve frame-invariance. In this regard, note that the differ-integral definition

of the nonlocal operator in the displacement-driven approach allows for a consistent definition for strain in the nonlocal material, analogous to classical continuum measures. This latter feature is not a characteristic of the peridynamic approach where the concept of strain is rather disjointed from the classical interpretation of strain, primarily due to the purely integral nature of the peridynamic nonlocal operator. As a result, the peridynamic nonlocal operator requires additional constraints to be imposed on the material model (more specifically, requires the material to be nonpolar in nature Silling and Lehoucq, 2010) in order to achieve frame-invariance. On the other hand, the nonlocal operator of the displacement-driven approach enables a straightforward treatment of frame-invariance irrespective of the nature of the underlying material model and of the kernel definition (see Section 3). From this perspective, the displacement-driven approach can be considered more general than the peridynamic approach.

· Finally, the consistent definition for the strain measure in the displacement-driven approach combined with the consistent behavior of the nonlocal operator at material boundaries also ensures a straightforward treatment of displacement boundary conditions analogous to the classical (local) continuum theory. On the other hand, the peridynamic approach requires the definition of an ad hoc region near the boundary (that is, a collection or set of points) for the application of the displacement boundary conditions (Silling, 2000). Notably, both the approaches result in nonlocal traction boundary conditions. While the traction boundary conditions are always incorporated within the equilibrium equations in the peridynamic approach, they require additional care in the displacement-driven approach depending on the chosen simulation technique. In this regard, we merely note that the nonlocal nature of the traction boundary conditions in the displacement-driven approach does not concern us immediately as we simulated the governing equations using a finite element technique. Recall that traction boundary conditions are implicitly satisfied when obtaining the solutions using finite element techniques and are accurate up to the order of the specific finite element method.

The above discussion highlighting the ability of the displacementdriven approach to model both softening and stiffening effects, nonlinear effects, and physical phenomena involving discontinuities, suggests that the displacement-driven approach presents a promising alternative to the analysis of nonlocal structures.

8. Conclusions

We presented an approach, that leverages strain-displacement relations formulated in a differ-integral form, to model nonlocal effects in an elastic solid. This method was dubbed as the displacementdriven approach to clearly differentiate it from the existing stressand strain-driven techniques. The mathematical, physical, and thermodynamic consistency of the method were carefully demonstrated, and shown to address some critical deficiencies of existing models of nonlocal elasticity. This approach may also be seen as a generalization of fractional-order formulations of nonlocal elasticity that restrict the nonlocal kernel to power-law type. The well-posedness of the elastic governing equations, which is a requisite for consistent modeling of elastic behavior, is achieved by the present approach. This observation is a direct consequence of the positive-definite and convex deformation energy density achieved by using the displacement-driven approach. The formulation also presents some other important benefits including the ability to adopt asymmetric kernels (required to capture from material heterogeneities), and the proper truncation of the nonlocal horizon at physical boundaries to maintain the completeness of the kernel. These features will be fundamental as nonlocal theories start

percolating into a broad spectrum of practical applications. We also derived the dispersion relations for a 1D infinite solid and showed the practical influence of some commonly used nonlocal kernels. It was found that different kernels capture different features of dynamic behavior, and hence their selection for dynamic analyses should be properly pondered. Finally, numerical simulations were performed to investigate the static response of nonlocal Timoshenko beams and nonlocal Mindlin plates. Numerical results highlighted the very consistent physical behavior enabled by the displacement-driven approach. This consistency was observed from the monotonic softening in the elastic response following an increase in the degree of nonlocality; a behavior observed irrespective of the choice of the nonlocal kernel, and of the loading and boundary conditions. In conclusion, the displacementdriven formulation provides a powerful framework to model nonlocal effects in elastic solids while enabling the use of different kernels that are representative of different dynamic material behavior.

CRediT authorship contribution statement

Sansit Patnaik: Conceptualization, Methodology, Software, Formal analysis, Writing – original draft, Visualization. Sai Sidhardh: Methodology, Software, Formal analysis, Writing – original draft, Visualization. Fabio Semperlotti: Conceptualization, Methodology, Formal analysis, Writing – original draft, Writing – review & editing, Visualization, Supervision, Project administration, Funding acquisition.

Declaration of competing interest

The authors declare that they have no known competing financial interests or personal relationships that could have appeared to influence the work reported in this paper.

Acknowledgments

The authors gratefully acknowledge the financial support of the National Science Foundation (NSF), United States under grants MOMS #1761423 and DCSD #1825837, and the Defense Advanced Research Project Agency (DARPA), United States under grant #D19AP00052. S.P. acknowledges the partial support received through the R. H. Kohr Graduate Fellowship from the School of Mechanical Engineering, Purdue University, United States. The content and information presented in this manuscript do not necessarily reflect the position or the policy of the government. The material is approved for public release; distribution is unlimited.

Appendix. Derivation of the strong-form of equilibrium equations

In the following, we present the details of the steps involved in the derivation of differ-integral (nonlocal) equilibrium equation for the nonlocal solid. For this purpose, we recall the Hamilton's principle in Eq. (28):

$$\int_{t_{1}}^{t_{2}} \delta \left[\frac{1}{2} \int_{\Omega} (\boldsymbol{\sigma} : \boldsymbol{\varepsilon}) d\mathbb{V} - \underbrace{\int_{\Omega} (\boldsymbol{\bar{b}} \cdot \boldsymbol{u}) d\mathbb{V} - \int_{\partial\Omega} (\boldsymbol{\bar{t}} \cdot \boldsymbol{u}) d\mathbb{A}}_{\text{External work}} \right]$$

$$- \underbrace{\frac{1}{2} \int_{\Omega} \rho(\boldsymbol{\dot{u}} \cdot \boldsymbol{\dot{u}}) d\mathbb{V}}_{\text{Kinetic energy}} dt = 0$$
(28)

The variations of the terms corresponding to the external work and kinetic energy are identical to their counterparts in local elasticity and hence, in the following, we will derive only the variation of the strain energy. By using the symmetry in the strain tensor, we express the variation of the strain energy as:

$$\mathcal{I}_{1} = \int_{t_{1}}^{t_{2}} \underbrace{\int_{\Omega} \sigma_{ij}(\mathbf{x}) \ \delta \overline{D}_{x_{j}} \left[u_{i}(\mathbf{x}) \right] d\mathbb{V}}_{I} dt$$
(51)

Now, by using the definition of the nonlocal operator $\overline{D}_{x_j}(\cdot)$ from Eq. (7), we obtain:

$$I_{2} = \int_{\Omega_{x_{i}}} \int_{\Omega_{x_{k}}} \int_{\Omega_{x_{j}}} \sigma_{ij}(\mathbf{x}) \left[c_{-j}^{*} \int_{x_{-j}}^{x_{j}} \mathcal{K}(\mathbf{x}, \mathbf{x}') \left[\frac{\mathrm{d}\delta u_{i}(x'_{j})}{\mathrm{d}x'_{j}} \right] \mathrm{d}x'_{j} \right] + c_{+j}^{*} \int_{x_{j}}^{x_{+j}} \mathcal{K}(\mathbf{x}, \mathbf{x}') \left[\frac{\mathrm{d}\delta u_{i}(x'_{j})}{\mathrm{d}x'_{j}} \right] \mathrm{d}x'_{j} \right] \mathrm{d}x_{j} \mathrm{d}x_{k} \mathrm{d}x_{i}$$
(52)

where, recall that, $x_{-j} = x_j - l_{-j}$ and $x_{+j} = x_j + l_{+j}$. Each of the two terms within the innermost integral in the above expression, can be re-written by changing the order of integration over the nonlocal spatial variable (x_j') and the local spatial variable along the same direction (x_j) . This gives:

$$I_{2} = \int_{\Omega_{x_{i}}} \int_{\Omega_{x_{k}}} \int_{\Omega_{x_{j}}} \left[\frac{\mathrm{d}\delta u_{i}(x_{j}')}{\mathrm{d}x_{j}'} \right] \left[c_{-j}^{*} \underbrace{\int_{x_{j}'}^{x_{j}'+l_{-j}} \mathcal{K}(\mathbf{x}, \mathbf{x}') \sigma_{ij}(\mathbf{x}) \mathrm{d}x_{j}}_{I_{x_{j}'}^{-} \left[\sigma_{ij}(x_{j}')\right]} + c_{+j}^{*} \underbrace{\int_{x_{j}'-l_{+j}}^{x_{j}'} \mathcal{K}(\mathbf{x}, \mathbf{x}') \sigma_{ij}(\mathbf{x}) \mathrm{d}x_{j}}_{I_{y}^{+} \left[\sigma_{ij}(x_{j}')\right]} \right] \mathrm{d}x_{j}' \mathrm{d}x_{k} \mathrm{d}x_{i}$$

$$(53)$$

Next, by denoting the convolutions of the nonlocal stress tensor as $I_{x_j'}^- \left[\sigma_{ij}(x_j')\right]$ and $I_{x_j'}^+ \left[\sigma_{ij}(x_j')\right]$, and using integration-by-parts to separate the variation from the displacement field, we obtain that:

$$I_{2} = -\int_{\Omega_{x_{i}}} \int_{\Omega_{x_{k}}} \int_{\Omega_{x_{j}}} \left[\delta u_{i}(x'_{j}) \right]$$

$$\times \left[\frac{\mathrm{d}}{\mathrm{d}x'_{j}} \left(c^{*}_{-j} I^{-}_{x'_{j}} \left[\sigma_{ij}(x'_{j}) \right] + c^{*}_{+j} I^{+}_{x'_{j}} \left[\sigma_{ij}(x'_{j}) \right] \right) \right] \mathrm{d}x'_{j} \mathrm{d}x_{k} \mathrm{d}x_{i}$$

$$+ \int_{\Omega_{x_{i}}} \int_{\Omega_{x_{k}}} \left[\delta u_{i}(x'_{j}) \right] \left[c^{*}_{-j} I^{-}_{x'_{j}} \left[\sigma_{ij}(x'_{j}) \right] + c^{*}_{+j} I^{+}_{x'_{j}} \left[\sigma_{ij}(x'_{j}) \right] \right] \Big|_{\partial \Omega_{x_{j}}} \mathrm{d}x_{k} \mathrm{d}x_{i}$$
(54)

By using the definition for $\tilde{I}_{x_j}(\cdot)$ given in Eq. (32), we obtain the following simplified expression for \mathcal{I}_2 :

$$I_{2} = -\int_{\Omega_{x_{i}}} \int_{\Omega_{x_{k}}} \int_{\Omega_{x_{j}}} \left[\delta u_{i}(x_{j}) \right] \left[\frac{\mathrm{d} \tilde{I}_{x_{j}} \sigma_{ij}(x_{j})}{\mathrm{d} x_{j}} \right] \mathrm{d} x_{j} \mathrm{d} x_{k} \mathrm{d} x_{i}$$

$$+ \int_{\Omega} \int_{\Omega} \left[\delta u_{i}(x_{j}) \right] \left[\tilde{I}_{x_{j}} \sigma_{ij}(x_{j}) \right] \Big|_{\partial \Omega_{x_{i}}} \mathrm{d} x_{k} \mathrm{d} x_{i}$$
(55)

Note that, in obtaining the above result, we interchanged the (dummy) variables x'_j and x_j , for the sake of brevity. Finally, by substituting the above result in Eq. (51), we obtain:

$$\mathcal{I}_{1} = \int_{t_{1}}^{t_{2}} \left[-\int_{\Omega} \left[\left(\widetilde{\mathbf{V}} \cdot \boldsymbol{\sigma} \right) \cdot \delta \boldsymbol{u} \right] d\mathbb{V} + \int_{\partial \Omega} \left[\left(\widetilde{\boldsymbol{I}}_{\hat{\boldsymbol{n}}} \cdot \boldsymbol{\sigma} \right) \cdot \delta \boldsymbol{u} \right] d\mathbb{A} \right] dt$$
 (56)

Applying the fundamental principle of variational calculus, we recover the governing equations in Eq. (29) and the boundary conditions in Eq. (30).

In order to summarize the variational simplifications performed above, we report below the variation of the nonlocal operator defined on the 1D space. This statement is more lean and hence, more transparent. The variation of the nonlocal operator defined in Eq. (6), on a finite-dimensional 1D space $\Omega_{\rm x} \in [0,L]$, is given as:

$$\int_{\Omega_{-}} f(x) \, \delta\left[\overline{D}_{x}g(x)\right] dx = -\int_{\Omega_{-}} \delta g(x) \left[\widetilde{D}_{x}f(x)\right] dx + \delta g(x) \left[\widetilde{I}_{x}f(x)\right] \Big|_{0}^{L} \tag{57}$$

where f(x) and g(x) are arbitrary functions. The definitions for $\tilde{I}_x(\cdot)$, and $\tilde{D}_x(\cdot)$ can be found in Eqs. (31)–(33). Note that the variational principle presented in Eq. (57), for the nonlocal operator defined in Eq. (6), is highly general since it is applicable irrespective of the definition of the nonlocal kernel. However, assuming a power-law kernel within the definition of the nonlocal operator (as a particular case) reduces the nonlocal operator to a fractional-order derivative, as mentioned in the discussion following Eq. (16). This special case also provides additional evidence in support of the above derived variational principle because it can be directly compared with results available in the literature of fractional-order variational calculus (see, for example, Patnaik et al., 2021b, 2020b; Agrawal, 2007; Atanacković et al., 2008; Almeida, 2012).

References

Agrawal, O.P., 2007. Fractional variational calculus in terms of Riesz fractional derivatives. J. Phys. A 40 (24), 6287.

Almeida, R., 2012. Fractional variational problems with the Riesz-Caputo derivative. Appl. Math. Lett. 25 (2), 142-148.

Alotta, G., Di Paola, M., Pinnola, F., Zingales, M., 2020. A fractional nonlocal approach to nonlinear blood flow in small-lumen arterial vessels. Meccanica 55, 891–906.

Ansari, R., Torabi, J., Norouzzadeh, A., 2018. Bending analysis of embedded nanoplates based on the integral formulation of Eringen's nonlocal theory using the finite element method. Physica B 534, 90–97.

Askari, E., Bobaru, F., Lehoucq, R., Parks, M., Silling, S., Weckner, O., 2008. Peridynamics for multiscale materials modeling. In: Journal of Physics: Conference Series, Vol. 125. IOP Publishing, 012078.

Askes, H., Aifantis, E.C., 2011. Gradient elasticity in statics and dynamics: An overview of formulations, length scale identification procedures, finite element implementations and new results. Int. J. Solids Struct. 48 (13), 1962–1990.

Atanacković, T., Konjik, S., Pilipović, S., 2008. Variational problems with fractional derivatives: Euler–Lagrange equations. J. Phys. A 41 (9), 095201.

Batra, R., 2021. Misuse of Eringen's nonlocal elasticity theory for functionally graded materials. Internat. J. Engrg. Sci. 159, 103425.

Bazant, Z.P., 1976. Instability, ductility, and size effect in strain-softening concrete. J. Eng. Mech. 102 (2), 331–344.

Bažant, Z.P., Chang, T.-P., 1984. Instability of nonlocal continuum and strain averaging. J. Eng. Mech. 110 (10), 1441–1450.

Buonocore, S., Sen, M., Semperlotti, F., 2019. Occurrence of anomalous diffusion and non-local response in highly-scattering acoustic periodic media. New J. Phys. 21 (3), 033011.

Carpinteri, A., Cornetti, P., Sapora, A., 2014. Nonlocal elasticity: An approach based on fractional calculus. Meccanica 49 (11), 2551–2569.

Challamel, N., Wang, C.M., 2008. The small length scale effect for a non-local cantilever beam: A paradox solved. Nanotechnology 19 (34), 345703.

Dell'Isola, F., Seppecher, P., Corte, A., 2015. The postulations á la D'Alembert and á la Cauchy for higher gradient continuum theories are equivalent: a review of existing results. Proc. R. Soc. A 471 (2183), 20150415.

Dell'Isola, F., Seppecher, P., Madeo, A., 2012. How contact interactions may depend on the shape of Cauchy cuts in Nth gradient continua: approach "à la D'Alembert". Z. Angew. Math. Phys. 63 (6), 1119–1141.

Di Paola, M., Failla, G., Pirrotta, A., Sofi, A., Zingales, M., 2013. The mechanically based non-local elasticity: An overview of main results and future challenges. Phil. Trans. R. Soc. A 371 (1993), 20120433.

Drapaca, C., Sivaloganathan, S., 2012. A fractional model of continuum mechanics. J. Elasticity 107 (2), 105–123.

Edelen, D.G., Laws, N., 1971. On the thermodynamics of systems with nonlocality. Arch. Ration. Mech. Anal. 43 (1), 24–35.

Eringen, A.C., 1972. Linear theory of nonlocal elasticity and dispersion of plane waves. Internat. J. Engrg. Sci. 10 (5), 425–435.

Eringen, A.C., 1983. On differential equations of nonlocal elasticity and solutions of screw dislocation and surface waves. J. Appl. Phys. 54 (9), 4703–4710.

Eringen, A.C., Edelen, D.G.B., 1972. On nonlocal elasticity. Internat. J. Engrg. Sci. 10

Eroglu, U., 2020. Perturbation approach to Eringen's local/non-local constitutive equation with applications to 1-D structures. Meccanica 55, 1119—1134.

Failla, G., Zingales, M., 2020. Advanced materials modelling via fractional calculus: Challenges and perspectives. Proc. R. Soc. Lond. Ser. A Math. Phys. Eng. Sci. 378, 20200050.

Fellah, Z.E.A., Berger, S., Lauriks, W., Depollier, C., 2004a. Verification of Kramers-Kronig relationship in porous materials having a rigid frame. J. Sound Vib. 270 (4–5), 865–885.

Fellah, Z.E.A., Chapelon, J.Y., Berger, S., Lauriks, W., Depollier, C., 2004b. Ultrasonic wave propagation in human cancellous bone: Application of Biot theory. J. Acoust. Soc. Am. 116 (1), 61–73.

- Fernández-Sáez, J., Zaera, R., Loya, J.A., Reddy, J.N., 2016. Bending of Euler–Bernoulli beams using Eringen's integral formulation: A paradox resolved. Internat. J. Engrg. Sci. 99, 107–116.
- Hollkamp, J.P., Semperlotti, F., 2020. Application of fractional order operators to the simulation of ducts with acoustic black hole terminations. J. Sound Vib. 465, 115035.
- Hollkamp, J.P., Sen, M., Semperlotti, F., 2019. Analysis of dispersion and propagation properties in a periodic rod using a space-fractional wave equation. J. Sound Vib. 441, 204–220.
- Kröner, E., 1967. Elasticity theory of materials with long range cohesive forces. Int. J. Solids Struct. 3 (5), 731–742.
- Lal, R., Dangi, C., 2019. Thermomechanical vibration of bi-directional functionally graded non-uniform Timoshenko nanobeam using nonlocal elasticity theory. Composites B 172, 724–742.
- Lazopoulos, K.A., 2006. Non-local continuum mechanics and fractional calculus. Mech. Res. Commun. 33 (6), 753–757.
- Lazopoulos, K., Lazopoulos, A., 2020. On plane Λ-fractional linear elasticity theory. Theor. Appl. Mech. Lett. 10 (4), 270–275.
- Lim, C., Zhang, G., Reddy, J., 2015. A higher-order nonlocal elasticity and strain gradient theory and its applications in wave propagation. J. Mech. Phys. Solids 78, 298–313.
- Magin, R.L., 2010. Fractional calculus models of complex dynamics in biological tissues. Comput. Math. Appl. 59 (5), 1586–1593.
- Mashayekhi, S., Miles, P., Hussaini, M.Y., Oates, W.S., 2018. Fractional viscoelasticity in fractal and non-fractal media: Theory, experimental validation, and uncertainty analysis. J. Mech. Phys. Solids 111, 134–156.
- Nair, S., 2019. Nonlocal Acoustic Black Hole Metastructures: Achieving Ultralow Frequency and Broadband Vibration Attenuation (Ph.D. thesis). Purdue University Graduate School.
- Patnaik, S., Jokar, M., Semperlotti, F., 2021a. Variable-order approach to nonlocal elasticity: Theoretical formulation, order identification via deep learning, and applications. Comput. Mech.
- Patnaik, S., Semperlotti, F., 2020a. A generalized fractional-order elastodynamic theory for non-local attenuating media. Proc. R. Soc. Lond. Ser. A Math. Phys. Eng. Sci. 476 (2238), 20200200.
- Patnaik, S., Semperlotti, F., 2021d. Variable-order fracture mechanics and its application to dynamic fracture. Npj Comput. Mater. 7 (1), 1-8.
- Patnaik, S., Sidhardh, S., Semperlotti, F., 2020b. A Ritz-based finite element method for a fractional-order boundary value problem of nonlocal elasticity. Int. J. Solids Struct. 202, 398–417.
- Patnaik, S., Sidhardh, S., Semperlotti, F., 2020c. Geometrically nonlinear analysis of nonlocal plates using fractional calculus. Int. J. Mech. Sci. 179, 105710.
- Patnaik, S., Sidhardh, S., Semperlotti, F., 2021b. Towards a unified approach to nonlocal elasticity via fractional-order mechanics. Int. J. Mech. Sci. 189, 105992.
- Patnaik, S., Sidhardh, S., Semperlotti, F., 2021c. Fractional-order models for the static and dynamic analysis of nonlocal plates. Commun. Nonlinear Sci. Numer. Simul. 95, 105601.
- Pisano, A.A., Fuschi, P., Polizzotto, C., 2021. Integral and differential approaches to Eringen's nonlocal elasticity models accounting for boundary effects with applications to beams in bending. ZAMM-J. Appl. Math. Mech./Z. Angew. Math. Mech. e202000152.
- Polizzotto, C., 2001. Nonlocal elasticity and related variational principles. Int. J. Solids Struct. 38 (42–43), 7359–7380.
- Polizzotto, C., Fuschi, P., Pisano, A., 2004. A strain-difference-based nonlocal elasticity model. Int. J. Solids Struct. 41 (9–10), 2383–2401.

- Polizzotto, C., Fuschi, P., Pisano, A., 2006. A nonhomogeneous nonlocal elasticity model. Eur. J. Mech. A Solids 25 (2), 308–333.
- Pradhan, S., Murmu, T., 2009. Small scale effect on the buckling of single-layered graphene sheets under biaxial compression via nonlocal continuum mechanics. Comput. Mater. Sci. 47 (1), 268–274.
- Rahimi, Z., Sumelka, W., Yang, X.-J., 2017. A new fractional nonlocal model and its application in free vibration of Timoshenko and Euler-Bernoulli beams. Eur. Phys. J. Plus 132 (11), 1–10.
- Reddy, J.N., 2003. Mechanics of Laminated Composite Plates and Shells: Theory and Analysis. CRC Press.
- Romano, G., Barretta, R., 2017. Nonlocal elasticity in nanobeams: the stress-driven integral model. Internat. J. Engrg. Sci. 115, 14–27.
- Romano, G., Barretta, R., Diaco, M., de Sciarra, F.M., 2017. Constitutive boundary conditions and paradoxes in nonlocal elastic nanobeams. Int. J. Mech. Sci. 121, 151–156.
- Romanoff, J., Karttunen, A.T., Varsta, P., Remes, H., Reinaldo Goncalves, B., 2020.
 A review on non-classical continuum mechanics with applications in marine engineering. Mech. Adv. Mater. Struct. 27 (13), 1065–1075.
- Romanoff, J., Reddy, J., 2014. Experimental validation of the modified couple stress Timoshenko beam theory for web-core sandwich panels. Compos. Struct. 111, 130–137.
- Shaat, M., Ghavanloo, E., Fazelzadeh, S., 2020. Review on nonlocal continuum mechanics: Physics, material applicability, and mathematics. Mech. Mater. 150, 103587.
- Sidhardh, S., Patnaik, S., Semperlotti, F., 2020. Geometrically nonlinear response of a fractional-order nonlocal model of elasticity. Int. J. Nonlinear Mech. 125, 103529.
- Sidhardh, S., Patnaik, S., Semperlotti, F., 2021a. Thermodynamics of fractional-order nonlocal continua and its application to the thermoelastic response of beams. Eur. J. Mech. A Solids 88, 104238.
- Sidhardh, S., Patnaik, S., Semperlotti, F., 2021b. Analysis of the post-buckling response of nonlocal plates via fractional-order continuum theory. J. Appl. Mech. 88, 1–22.
- Sidhardh, S., Ray, M.C., 2018. Effect of nonlocal elasticity on the performance of a flexoelectric layer as a distributed actuator of nanobeams. Int. J. Mech. Mater. Design 14 (2), 297–311.
- Silling, S.A., 2000. Reformulation of elasticity theory for discontinuities and long-range forces. J. Mech. Phys. Solids 48 (1), 175–209.
- Silling, S.A., Lehoucq, R.B., 2010. Peridynamic theory of solid mechanics. Adv. Appl. Mech. 44, 73-168.
- Sumelka, W., 2014. Thermoelasticity in the framework of the fractional continuum mechanics. J. Therm. Stresses 37 (6), 678–706.
- Sumelka, W., 2017. On fractional non-local bodies with variable length scale. Mech. Res. Commun. 86, 5–10.
- Trovalusci, P., De Bellis, M.L., Masiani, R., 2017. A multiscale description of particle composites: From lattice microstructures to micropolar continua. Composites B 128,
- Trovalusci, P., De Bellis, M.L., Ostoja-Starzewski, M., Murrali, A., 2014. Particulate random composites homogenized as micropolar materials. Meccanica 49 (11), 2719–2727.
- Tuna, M., Kirca, M., Trovalusci, P., 2019. Deformation of atomic models and their equivalent continuum counterparts using Eringen's two-phase local/nonlocal model. Mech. Res. Commun. 97, 26–32.
- Wang, C.Y., Murmu, T., Adhikari, S., 2011. Mechanisms of nonlocal effect on the vibration of nanoplates. Appl. Phys. Lett. 98 (15), 153101.
- Zhu, H., Patnaik, S., Walsh, T.F., Jared, B.H., Semperlotti, F., 2020. Nonlocal elastic metasurfaces: Enabling broadband wave control via intentional nonlocality. Proc. Natl. Acad. Sci. 117 (42), 26099–26108.